Elsevier Editorial System(tm) for
International Journal of Solids and Structures
Manuscript Draft

Manuscript Number: IJSS-D-16-00986R1

Title: Complex bifurcation maps in electroelastic elastomeric plates.

Article Type: Research paper

Keywords: elastomers; electroactive materials; bifurcations; instabilities; Mooney-Rivlin model; Ogden model

Corresponding Author: Dr. Ricardo Diaz-Calleja,

Corresponding Author's Institution: Universitat Politècnica de València

First Author: Ricardo Diaz-Calleja

Order of Authors: Ricardo Diaz-Calleja; Pedro LLovera-Segovia, PhD; Alfredo Quijano-López, PhD

Abstract: Stress-strain relationships for rubbery materials are highly non-linear. In this work, a particular configuration of electroactive material is considered: an isotropic, incompressible electroelastic squared plate is subjected to equal biaxial homogeneous deformation and a scalar electrical potential is applied on the sides of compliant electrodes. This case is analysed according to two methodologies: the Hessian approach and the use of incremental deformation together with increment in the electric displacement. First, an extended Mooney-Rivlin model is considered for the material and then an Ogden model is also analysed. Results, show, that despite of available experimental results, some predictions can be made and the pertinent analysis show complex bifurcation maps. This can help in the future progress in the knowledge of the instabilities and bifurcation phenomena which should appear in these materials. The present paper has been mainly motivated by the work of Ogden and Dorfmann.

*Highlighted Revision

Complex bifurcation maps in electroelastic elastomeric plates.

R. Díaz-Calleja, P. Llovera-Segovia, A. Quijano-López.

ITE, Universitat Politècnica de València, Cº Vera s/n, E-46022, Valencia (Spain)-Instituto Tecnológico de la Energía-Redit.

Abstract.

Stress-strain relationships for rubbery materials are highly non-linear. In this work, a particular configuration of electroactive material is considered: an isotropic, incompressible electroelastic squared plate is subjected to equal biaxial homogeneous deformation and a scalar electrical potential is applied on the sides of compliant electrodes. This case is analysed according to two methodologies: the Hessian approach and the use of incremental deformation together with increment in the electric displacement. First, an extended Mooney-Rivlin model is considered for the material and then an Ogden model is also analysed. Results, show, that despite of available experimental results, some predictions can be made and the pertinent analysis show complex bifurcation maps. This can help in the future progress in the knowledge of the instabilities and bifurcation phenomena which should appear in these materials. The present paper has been mainly motivated by the work of Ogden and Dorfmann.

1. Introduction.

Stress-strain relationships for rubbery materials are highly non-linear. As a consequence, solutions of many traction boundary problems are not unique. Concomitantly, due to the nonconvexity of the free energy function, instability and bifurcation phenomena appear giving rise to problems in the design of sensor and actuators devices. For this reason, the analysis of these phenomena in these electroactive elastomers is compulsory in order to have a better understanding of the actual behaviour of these materials and avoid undesirable unstable behaviour.

Instabilities in thin plates of electroelastic materials have been theoretically predicted by using homogeneous deformations and regardless of the thickness of the plates. The Hessian approach has been used in the current literature to analyse these instabilities [1-12]. By contrast, the use of incremental deformation together with increment in the electric displacement has revealed to be a more powerful tool to analyse the case where non-homogeneous deformations and plate thickness are considered [13, 14]. In these circumstances the inherent formal treatment requires, in general, new material parameters implying a more complex analysis. However, due to the scarcity of experimental knowledge of these parameters, a detailed characterization of the unstable behaviour of these electroactive elastomers is not possible at present.

In spite of that, some predictions can be made in some particular cases and the pertinent analysis show complex bifurcation maps. This can help in the future progress in the knowledge of the instabilities and bifurcation phenomena which should appear in these materials. The present paper has been mainly motivated by the work of Ogden and Dorfmann [13, 14, 15] which is briefly summarized in Appendix A. In fact, the main target of the present study is to extend the study of the instability and bifurcation made in Ref. [13, 14] by applying more realistic electroelastic models than the neo-Hookean one. In the pertinent analysis of the problem new facts appear that merit consideration.

2. Geometry, finite deformation and incremental formulation.

Thus, in the spirit of Dorfmann and Ogden [14], an isotropic, incompressible electroelastic squared plate is subjected to equal biaxial homogeneous deformation and a scalar electrical potential is applied on the sides of compliant electrodes. Specifically, let us assume a plate of initial thickness H subjected to a plane strain biaxial stretch in the directions 1, 3 and a normal electric force field in the direction 2. The plate will be considered to be bounded by flexible (compliant) electrodes. Thus, it will be assumed that no electric field exists outside the plate (see App. A). The continuity condition applied to the boundary $x_2 = h$ (being h the actual thickness of the plate) under incompressibility condition gives $D_{L2} = -\sigma_F$. where D_{L2} is the Lagrangian component of the electric displacement (see Eq. A7).

In the general case, if $\lambda_1, \lambda_2, \lambda_3$ are the principal stretches, the invariants are

$$I_1 = \lambda_1^2 + \lambda_3^2 + \lambda_1^{-2}\lambda_3^{-2}, \quad I_2 = \lambda_1^{-2} + \lambda_3^{-2} + \lambda_1^2\lambda_3^2,$$

$$I_4 = D_{L2}^2, I_5 = \lambda_1^{-2}\lambda_3^{-2}D_{L2}^2, \quad I_6 = \lambda_1^{-4}\lambda_3^{-4}D_{L2}^2 \tag{1}$$

In this case, the principal stresses and the electric field are

$$\tau_{11} = \lambda_1 \frac{\partial \Omega^*}{\partial \lambda_1} - p^*$$

$$\tau_{33} = \lambda_3 \frac{\partial \Omega^*}{\partial \lambda_2} - p^*$$

$$\tau_{22} = \lambda_2 \frac{\partial \Omega^*}{\partial \lambda_3} - p^* + 2\Omega_5^* \lambda_1^{-2}\lambda_3^{-2} D_{L2}^2 + 4\Omega_6^* \lambda_1^{-4}\lambda_3^{-4} D_{L2}^2$$

$$E_2 = E_{L2}\lambda_2^{-1} = 2(\Omega_4^*\lambda_2^{-1} + \Omega_5^*\lambda_2 + \Omega_6^*\lambda_2^3)D_{L2} \quad (2)$$

where p^* is a Lagrange multiplier becoming from the incompressibility condition and Ω^* is the free energy density and Ω_i^* is defined as $\frac{\partial \Omega^*}{\partial I_i}$ for $i = 1,2,4,5,6$.

The elimination of p^*leads to

$$\tau_{11} - \tau_{22} = \lambda_1 \frac{\partial \widehat{\Omega}^*}{\partial \lambda_1} - 2\widehat{\Omega}_5^* \lambda_1^{-2}\lambda_3^{-2} D_{L2}^2 - 4\widehat{\Omega}_6^* \lambda_1^{-4}\lambda_3^{-4} D_{L2}^2$$

$$\tau_{33} - \tau_{22} = \lambda_3 \frac{\partial \widehat{\Omega}^*}{\partial \lambda_3} - 2\widehat{\Omega}_5^* \lambda_1^{-2}\lambda_3^{-2} D_{L2}^2 - 4\widehat{\Omega}_6^* \lambda_1^{-4}\lambda_3^{-4} D_{L2}^2 \quad (3)$$

where the free energy has been redefined as $\widehat{\Omega}^*(\lambda_1, \lambda_3, I_4, I_5, I_6)$.

For the incompressibility condition and Eq. (1), only three independent variables remain. Thus, let us take these to be $\lambda_1, \lambda_3, D_{L2}$ and define $\widetilde{\Omega}^*$ where $\widetilde{\Omega}^*(\lambda_1, \lambda_3, D_{L2}) = \widehat{\Omega}^*(\lambda_1, \lambda_3, I_4, \lambda_2^2 I_4, \lambda_2^4 I_4)$ is a new reduced form of the free energy density taken into account that only three independent variables $\lambda_1, \lambda_3, D_{L2}$ remain in the problem.

Now, it is assumed that the plate is bounded by flexible (compliant) electrodes on $x_2 = 0, h$ and free surface charges $-\sigma_f, \sigma_f$ per unit area are placed, respectively, on each electrode.

If no traction exists on the faces then $\tau_{22} = 0$ and two first equations of (3) simplify to

$$\lambda_1 T_{11} = \tau_{11} = \lambda_1 \frac{\partial \widetilde{\Omega}^*}{\partial \lambda_1}, \quad \lambda_3 T_{33} = \tau_{33} = \lambda_3 \frac{\partial \widetilde{\Omega}^*}{\partial \lambda_3}, \quad (4)$$

and $E_2 = \lambda_2^{-1} \frac{\partial \widetilde{\Omega}^*}{\partial D_{L2}}$.

where T_{11} and T_{33} are the nominal stress components.

If the potential difference between the electrodes is V and the electric field is uniform then $V = E_2 h = E_{L2} H$ and $h = \lambda_1 \lambda_3 H$.

For equibiaxial deformations $\lambda_1 = \lambda_3 = \lambda$, which implies $\lambda_2 = \lambda^{-2}$, one can define a reduced form of the energy function $\omega^* = \omega^*(\lambda, D_{L2})$. In this case, the two non-zero components of the stress are $\tau_{11} = \tau_{33} = \tau$, where

$$\tau = \frac{1}{2}\lambda \frac{\partial \omega^*}{\partial \lambda} = 2(\Omega_1^* + \lambda^2 \Omega_2^*)(\lambda^2 - \lambda^{-4}) - 2\Omega_5^* D_2^2 - 4\Omega_6^* \lambda^{-4} D_2^2 \quad (5)$$

and Ω_i^* denotes the derivative of the free energy with respect to I_i and $D_2 = \lambda^{-2} D_{L2}$ relating the Eulerian and Lagrangian electric displacement.

From the preceding equations an analysis of the stability can be outlined as in Ref. [1-12]. However, to fully analyze the stability of electroelastic plates the possibility of non-homogeneous deformations and the dependence on the plate thickness can´t be ruled out. Consequently, in the remaining part of the paper an incremental strategy has been outlined as in Ref. [14]. The basic idea underlying the incremental formulation is to use small deformations and electric displacements superimposed on a known large deformation [16]. The pertinent details are summarized in Appendix B.

3. Extended Mooney-Rivlin model.

In order to consider a more general model than the neo-Hookean one, let us assume the following expression for the free energy that generalizes Eq. (5)

$$\omega^*(\lambda, m, D_{L2}) = \Omega_1^*\Big[((I_1-3)+(I_2-3)h^*)+\frac{1}{2}m\Omega_1^*((I_1-3)+(I_2-3)h^*)^2+\frac{1}{2\epsilon_0\Omega_1^*}\beta\lambda^{-4}D_{L2}^2\Big] \tag{6}$$

where $h^* = \Omega_2^*/\Omega_1^*$ and $I_1 = 2\lambda^2+\lambda^{-4}$, $I_2 = 2\lambda^{-2}+\lambda^4$

In eq. (6), m is a parameter affecting the second order term of the expansion in powers of the Mooney-Rivlin free energy density$(\Omega_1^*(I_1-3)+\Omega_2^*(I_2-3))$. In fact this equation generalizes the electroactive Mooney-Rivlin equation to include quadratic terms in the mechanical invariants. This generalization is, of course, a possible one among many others and has been chosen for illustrative purposes. The parameter is defined from Eq. (5) as $\beta = 2\Omega_5^*$. Eq. (6) implies that the permittivity is deformation independent and in this case β^{-1} can be interpreted as the relative permittivity. Concomitantly, the invariant I_6 is excluded in the proposed constitutive model. Moreover, if one makes $h^* = 0$ in Eq. (6), then the resulting constitutive equation is similar to the so-called equation for an “ideal dielectric elastomer” by Zhao and Suo [2].

Since no traction is present on the faces, $\tau_{22} = 0$ and from Eq. (5), the lateral stress is given by

$$\tau = 2\Omega_1^*\{[(\lambda^2-\lambda^{-4})(1+h^*\lambda^2)(1+m\Omega_1^*((I_1-3)+(I_2-3)h^*))]-\beta\widehat{D}_2^2\} \tag{7}$$

where $\widehat{D}_2 = \frac{D_2}{(2\Omega_1^*\varepsilon_0)^{\frac{1}{2}}}$

If no lateral traction is present, Eq. (7) leads to

$$\widehat{D}_2^2 = \beta^{-1}[(\lambda^2-\lambda^{-4})(1+h^*\lambda^2)(1+m\Omega_1^*((I_1-3)+(I_2-3)h^*))] \tag{8}$$

Since Ω_1^* and h^* and the relative permittivity are currently positive, if $m > 0$ the plate becomes thinner when the electric field increases.

Incremental equations include expressions for the tensors $\boldsymbol{\mathcal{A}}_{\mathbf{0}}^*, \mathbb{A}_{\mathbf{0}}^*, \boldsymbol{A}$ in terms of the first and second order derivatives of Ω^* with respect to the invariants (see App. B). Then, the material parameters given by Eq. (B14) for our incompressible material under biaxial stretching can be calculated by means of the Eq. (40-51) of Ref. [13].

Results are

$$a = 2\Omega_1^*\lambda^2(1 + h^*\lambda^2)(1 + m\Omega_1^*((I_1 - 3) + (I_2 - 3)h^*))$$

$$2b = 2\Omega_1^*[(\lambda^2 + \lambda^{-4})(1 + h^*\lambda^2)(1 + m\Omega_1^*((I_1 - 3) + (I_2 - 3)h^*))] + 4m{\Omega_1^*}^2(1 + h^*\lambda^2)^2(\lambda^2 - \lambda^{-4})^2 + 2\varepsilon_0^{-1}\beta D_2^2$$

$$c = 2\Omega_1^*\lambda^{-4}(1 + h^*\lambda^2)(1 + m\Omega_1^*((I_1 - 3) + (I_2 - 3)h^*)) + 2\varepsilon_0^{-1}\beta D_2^2$$

$$d = 2\varepsilon_0^{-1}\beta D_2$$

$$e = 4\varepsilon_0^{-1}\beta D_2$$

$$f = g = 2\varepsilon_0^{-1}\beta \qquad (9)$$

Then, the bi-cubic equation (B16) can be solved to give

$$s_1 = -s_2 = 1$$

$$s_3 = -s_4 = \frac{1}{2^{1/2}}\left\{\left(\lambda^6 + 1 + \frac{2m\lambda^{-4}(\lambda^6 - 1)^2(1 + h^*\lambda^2)}{1 + m\Omega_1^*((I_1 - 3) + (I_2 - 3)h^*)}\right) - \left[\left(\lambda^6 + 1 + \frac{2m\lambda^{-4}(\lambda^6 - 1)^2(1 + h^*\lambda^2)}{1 + m\Omega_1^*((I_1 - 3) + (I_2 - 3)h^*)}\right)^2 - 4\lambda^6\right]^{\frac{1}{2}}\right\}^{\frac{1}{2}}$$

$$s_5 = -s_6 = \frac{1}{2^{1/2}}\left\{\left(\lambda^6 + 1 + \frac{2m\lambda^{-4}(\lambda^6 - 1)^2(1 + h^*\lambda^2)}{1 + m\Omega_1^*((I_1 - 3) + (I_2 - 3)h^*)}\right) + \left[\left(\lambda^6 + 1 + \frac{2m\lambda^{-4}(\lambda^6 - 1)^2(1 + h^*\lambda^2)}{1 + m\Omega_1^*((I_1 - 3) + (I_2 - 3)h^*)}\right)^2 - 4\lambda^6\right]^{\frac{1}{2}}\right\}^{\frac{1}{2}}$$

(10)

Note that in these equations the electric displacement is absent. This is a consequence of the hypothesis $\alpha = 0$. In the case where $\alpha \neq 0$ no solutions $s_1 = -s_2 = 1$ of Eq. (16) appear what makes much more involved the solution of the present problem.

In the following developments the dimensionless variable

$$\hat{B}_j = \frac{B_j}{(2\Omega_1^*\varepsilon_0)^{\frac{1}{2}}} \qquad (11)$$

is introduced.

Substitution of Eq. (10, 11) in Eq. (B22), leads to

$\sum_{j=1}^{6}\left[\left(\lambda^{-4}(1+h^*\lambda^2)(1+m\Omega_1^*((I_1-3)+(I_2-3)h^*))+\widehat{D}_2^2\right)\left(1+s_j^2\right)A_j-\widehat{D}_2 s_j\widehat{B}_j\right]=0$

$\sum_{j=1}^{6}\{[(\lambda^2+2\lambda^{-4})(1+h^*\lambda^2)(1+m\Omega_1^*((I_1-3)+(I_2-3)h^*))+2m\Omega_1^*\lambda^4(1+$
$h^*\lambda^2)^2(1-\lambda^{-6})^2+\widehat{D}_2^2-\left[\lambda^{-4}(1+h^*\lambda^2)(1+m\Omega_1^*((I_1-3)+(I_2-3)h^*))+\right.$
$\left.\widehat{D}_2^2\right]s_j^2]s_jA_j-\widehat{D}_2(2-s_j^2)\widehat{B}_j]\}=0$

$\sum_1^6\left[\widehat{D}_2\left(1+s_j^2\right)A_j-s_j\widehat{B}_j\right]=0$

$\sum_{j=1}^{6}\left[\left(\lambda^{-4}(1+h^*\lambda^2)(1+m\Omega_1^*((I_1-3)+(I_2-3)h^*))+\widehat{D}_2^2\right)\left(1+s_j^2\right)A_j-\right.$
$\left.\widehat{D}_2 s_j\widehat{B}_j\right]e^{-ks_jh}=0$

$\sum_{j=1}^{6}\{[(\lambda^2+2\lambda^{-4})(1+h^*\lambda^2)(1+m\Omega_1^*((I_1-3)+(I_2-3)h^*))+2m\Omega_1^*\lambda^4(1+$
$h^*\lambda^2)^2(1-\lambda^{-6})^2+\widehat{D}_2^2-\left[\lambda^{-4}(1+h^*\lambda^2)(1+m\Omega_1^*((I_1-3)+(I_2-3)h^*))+\right.$
$\left.\widehat{D}_2^2\right]s_j^2]s_jA_j-\widehat{D}_2(2-s_j^2)\widehat{B}_j]\}e^{-ks_jh}=0$

$\sum_1^6\left[\widehat{D}_2\left(1+s_j^2\right)A_j-s_j\widehat{B}_j\right]e^{-ks_jh}=0$ (12)

where in the biaxial stretching case $h=\lambda^{-2}H$ and A_j and $\widehat{B}_j$ are defined in Eq. (B17). .

In the same way, Eq. (B18) leads to the following relationship between A_j and $\widehat{B}_j$

$(s_j^2-1)(s_j\widehat{D}_2A_j-\widehat{B}_j)=0$ (13)

Thus, if in (13) $s_j=\pm1, \widehat{B}_j\neq s_j\widehat{D}_2A_j$ (in general)

$s_j\neq\pm1, \widehat{B}_j=s_j\widehat{D}_2A_j$ (14)

Incidentally, note that if one takes $m=0$ the equation (13) reduces to

$(s^2-1)^2(s^2-\lambda^6)=0$ (15)

and one returns to the extended Mooney-Rivlin model.

Eq. (13) and (14) indicate that only when $s_j, j=3,\ldots,6$ there exists a connection between A_j and $\widehat{B}_j$ whereas for $s_j, j=1{,}2$ such relation is undetermined and consequently the system of six homogeneous equations (12) has eight unknowns $A_j, j=1,\ldots,6, \widehat{B}_{j,}\ j=1{,}2$. It can be shown that if one assumes $\widehat{B}_j=s_j\widehat{D}_2A_j$ for $j=1{,}2$ then the bifurcation map is independent of the applied electric field that seems an inconsistent result. For this reason it will be taken $\widehat{B}_j=0,\ j=1{,}2$. This implies to modify the proposed solution for φ (cf. Eq. (B17)$_2$), that is,

$\varphi=k\sum_{j=3}^{6}B_j\exp\left(-ks_jx_2\right)\exp(ikx_1)$ (16)

With these premises, the homogeneous system (12) results in a system of 6 equations with 6 unknowns and the corresponding determinant must vanish as usual for a non trivial solution.

This determinant is equalized to zero in order to identify the critical pre-stretch values $\lambda_{crit.}$ announcing the unstable behavior.

It is noticeable that the parameter m in Eq. (6) could be either positive or negative, for, respectively positive or negative deviations of the Mooney-Rivlin mechanical behaviour. As mentioned above, if m is positive, the function represented by Eq. (8) is increasing with λ and the plate thins with increasing the applied electric force field. However, if m is negative the situation is more complex. In order to compare the results with those of Ref. [14] one will take in the calculations that follow $\beta = 0.5$. Accordingly, in Figure 1 a plot of $\widehat{D}_2$ vs. λ for $\beta = 0.5$ and different values of $m\Omega_1^*$is shown. This plot indicates that for decreasing values of $m\Omega_1^*$ the plate tends to be more unstable and determines the limits of stability for the system under study. For this reason, only small negative values for $m\Omega_1^*$ seems to be physically reasonable. In order to be more specific in Figure 2 values of $m\Omega_1^*$ vs. λ for the chosen $\beta = 0.5$ and different applied electric fields are shown.

In absence of electric field, and according to the Eq. (9) and (B24), one obtains

$$s_1 = -s_2 = \frac{1}{2^{1/2}}\left\{\begin{array}{c}\left(\lambda^6 + 1 + \frac{2m\lambda^{-4}\left(\lambda^6-1\right)^2\left(1+h^*\lambda^2\right)}{1+m\Omega_1^*((I_1-3)+(I_2-3)h^*)}\right)\\ - \\ \left[\left(\lambda^6 + 1 + \frac{2m\lambda^{-4}\left(\lambda^6-1\right)^2\left(1+h^*\lambda^2\right)}{1+m\Omega_1^*((I_1-3)+(I_2-3)h^*)}\right)^2 - 4\lambda^6\right]^{\frac{1}{2}}\end{array}\right\}^{\frac{1}{2}}$$

$$s_3 = -s_4 = \frac{1}{2^{1/2}}\left\{\begin{array}{c}\left(\lambda^6 + 1 + \frac{2m\lambda^{-4}\left(\lambda^6-1\right)^2\left(1+h^*\lambda^2\right)}{1+m\Omega_1^*((I_1-3)+(I_2-3)h^*)}\right)\\ + \\ \left[\left(\lambda^6 + 1 + \frac{2m\lambda^{-4}\left(\lambda^6-1\right)^2\left(1+h^*\lambda^2\right)}{1+m\Omega_1^*((I_1-3)+(I_2-3)h^*)}\right)^2 - 4\lambda^6\right]^{\frac{1}{2}}\end{array}\right\}^{\frac{1}{2}} \quad (17)$$

which are the four roots differing of $s_{1,2} = \pm 1$ in Eq. (10).

Also note that in the absence of electric force field the bicubic equation [B16] reduces to a bicuadratic one and, in this case, one has

$$cs^4 - 2bs^2 + a = 0 \quad (18)$$

where a,b,c are given by

$$a = 2\Omega_1^*\lambda^2(1 + h^*\lambda^2)(1 + m\Omega_1^*((I_1 - 3) + (I_2 - 3)h^*))$$

$$b = \Omega_1^*[(\lambda^2 + \lambda^{-4})(1 + h^*\lambda^2)(1 + m\Omega_1^*((I_1 - 3) + (I_2 - 3)h^*))] + 4m{\Omega_1^*}^2(1 + h^*\lambda^2)^2(\lambda^2 - \lambda^{-4})^2$$

$$c = 2\Omega_1^*\lambda^{-4}(1 + h^*\lambda^2)(1 + m\Omega_1^*((I_1 - 3) + (I_2 - 3)h^*)) \quad (19)$$

The solutions of Eq. (18) are

$$s = \pm\left[\frac{b \pm (b^2 - ac)^{1/2}}{c}\right]^{1/2} \tag{20}$$

Then, on account of the relationship between A_j and B_j $(14)_1$ the problem reduces to examine the determinant of a 4x4 matrix corresponding to a system of four homogeneous equations with four unknowns.

3.1. Results and discussion.

In Figure 3, plots of $\lambda_{cr.}$ vs. *kH* with $m\Omega_1^* = 0.01$ and $h^* = 0.2$ for different values of the applied electric field are shown. The characteristic curves corresponding to the different modes of deformation tend to merge together for large values of *kH* and these values increase with the electric field. Moreover an upper branch that increases with *kH* appears. Figure 3a illustrates the case where the applied electric field is absent. In this particular case, the limiting value for $kH \to \infty$ is $\lambda_{cr.} \cong 0.6661$.

In general, for moderate electric fields, the plate becomes unstable for values of the lateral stretch below the upper curve but above the lower one. Thus, in order to prevent a loss of stability, the lateral stretch should be increased as the electric field increases. However, for larger electric fields the situation becomes more complex and, for example, the bifurcation map for $\widehat{D}_2 = 2$ and *kH*=2 show alternative zones of stability and instability with increasing values of $\lambda_{cr.}$. In the case of values of $\widehat{D}_2 > 3$ the bifurcation map simplifies showing a small unstable region which tends to diminish for progressively larger values of the electric field together with a upper branch that increases with the electric field. For $\widehat{D}_2 = 5$, the unstable region is confined to a maximum value of $\lambda_{ct.} = 0.62$ and *kH* less than the unity. At the same time the upper curves show a relatively small slope and move to higher values of critical stretches with increasing the electric field.

In a similar way, Figure 4 shows plots of $\lambda_{ct.}$ vs. *kH* with $m\Omega_1^* = -0.01$ and $h^* = 0.2$ for different values of the applied electric field. In the present case, the bifurcation map is fairly more complex. Figure 4a corresponds to the case where the electric field is absent. In this case, the merging value for the critical stretch is 0.6715. It is to be noted that for values of $\lambda_{cr.} \leq 0.428$ and $\lambda_{cr.} \geq 3.16$ the plots are meaningless due to the fact that, taking $m\Omega_1^* = -0.01$, for these values of the stretch, imaginary values of s in Eq. (17) are obtained. For a similar reason, the curves corresponding to the situation when the electric field is present, do not show indication below about $\lambda_{cr.} = 0.5$. In general, for moderate electric fields the unstable zones tend to decrease for vales of *kH* between 4 and 5 and for higher values of *kH* these zones tend to be open giving rise to a new unstable zone. For $\widehat{D}_2 = 1$ the first unstable zone closes at about kH=5.5 and the second unstable zone becomes more complex. For values of $\widehat{D}_2$ between 1.5 and 1.9 new stable zones appear above and below $\lambda_{cr.} = 1$ which for $\widehat{D}_2 > 2$ induce a broad zone of stability which increases to about $\widehat{D}_2 = 2.25$. For higher values of the electric field the stable region tends to diminish.

If one makes $m = 0$ in Eq. (6) the density of the free energy is given by

$$\omega^*(\lambda, D_3) = \Omega_1^* \left[(2\lambda^2 + \lambda^{-4} - 3) + h^*(2\lambda^{-2} + \lambda^4 - 3) + \frac{\beta}{2\varepsilon_0 \Omega_1^*} D_3^2\right] \qquad (21)$$

where, as above, $h^* = \frac{\Omega_2^*}{\Omega_1^*}$ (recalling that $D_3 = \lambda^{-2} D_{L3}$).

then Eq. (12) reduces to

$$\sum_{j=1}^{6}\left[(\lambda^{-4}(1 + h^*\lambda^2) + \widehat{D}_2^2)\left(1 + s_j^2\right)A_j - \widehat{D}_2 s_j \hat{B}_j\right] = 0$$

$$\sum_{j=1}^{6}\left\{\left[(\lambda^2 + 2\lambda^{-4})(1 + h^*\lambda^2) + \widehat{D}_2^2 - \left[\lambda^{-4}(1 + h^*\lambda^2) + \widehat{D}_2^2\right]s_j^2\right]s_j A_j - \widehat{D}_2(2 - s_j^2)\hat{B}_j\right]\right\} = 0$$

$$\sum_{1}^{6}\left[\widehat{D}_2\left(1 + s_j^2\right)A_j - s_j \hat{B}_j\right] = 0$$

$$\sum_{1}^{6}\left[(\lambda^{-4}(1 + h^*\lambda^2) + \widehat{D}_2^2)\left(1 + s_j^2\right)A_j - \beta\widehat{D}_2 s_j \hat{B}_j\right] e^{-ks_j h} = 0$$

$$\sum_{j=1}^{6}\left\{\left[(\lambda^2 + 2\lambda^{-4})(1 + h^*\lambda^2) + \widehat{D}_2^2 - \left[\lambda^{-4}(1 + h^*\lambda^2) + \widehat{D}_2^2\right]s_j^2\right]s_j A_j - \widehat{D}_2(2 - s_j^2)\hat{B}_j\right]\right\}e^{-ks_j h} = 0$$

$$\sum_{1}^{6}\left[\widehat{D}_2\left(1 + s_j^2\right)A_j - s_j \hat{B}_j\right]e^{-ks_j h} = 0$$

(22)

and the roots of Eq. (13) give

$$s_1 = 1\ (double),\ s_2 = -1\ (double),\ s_3 = \lambda^3,\ s_3 = -\lambda^3 \qquad (23)$$

Then, according to the strategy outlined in [14], the corresponding bifurcation equation is obtained and subsequently the bifurcation maps.

In Figure 5, plots of $\lambda_{crit.}$ vs. kH are shown. As expected, these plots are close to those of Figure 3 of Ref. [14].

It should be noted that when the electric field is absent, $\left(\widehat{D}_2 = 0\right)$, the factor $(1 + h^* \lambda^2)$ cancel in the main equations, the matrix obtained to find the unstable zones is reduced to a 4x4 one and the corresponding stability plot is exactly the obtained in Figure 3a of [14]. In this case, the equation giving the bifurcation map obtained from the cancellation of the corresponding determinant can be easily evaluated in a closed form to give

$$[16\lambda^6 + (\lambda^6 + 1)^4] \sinh(kH) \sinh(kH\lambda^3) - 8\lambda^3(\lambda^6 + 1)^2(\cosh(kH)\cosh(kH\lambda^3) - 1) \tag{24}$$

It is noticeable that since the term $(1 + h^* \lambda^2)$ is specifically due to the two parameter Mooney-Rivlin model, the cancellation of this factor reduces the stability behaviour and the bifurcation map to that obtained by using the neo-Hookean model. This conclusion is the opposite when the study of the stability and bifurcation phenomena of a square plate is set in terms of two equal biaxial forces in the 1 and 3 directions also in the absence of electric field [17]. This fact reveals not only the significant differences in the predictions of the two methods of analysis considered in this paper, but also the different results obtained when the sample is attacked by tension instead of deformation.

3.2. Comparison with the Hessian approach.

It is interesting to compare the preceding results with those obtained via the hessian approach. For equibiaxial deformation the Hessian matrix is given by

$$\begin{bmatrix} \frac{\partial^2 \omega^*}{\partial \lambda^2} & \frac{\partial^2 \omega^*}{\partial \lambda \partial D_{L2}} \\ \frac{\partial^2 \omega^*}{\partial D_{L2} \partial \lambda} & \frac{\partial^2 \omega^*}{\partial D_{L2}^2} \end{bmatrix} \tag{25}$$

The system is stable if the determinant of the Hessian matrix is positive.

From the Eq. (6) the determinant of the matrix (25) leads to

$$8{\Omega_1^*}^2 \beta \lambda^{-4}[(\lambda^6 + 5) + 3h^*(\lambda^8 + \lambda^2) + m\Omega_1^* \Big((6\lambda^8 - 3\lambda^6 + 3\lambda^2 + 9\lambda^{-4} - 15) + h^*(15\lambda^{10} - 9\lambda^8 - 3\lambda^6 - 9\lambda^2 + 21\lambda^{-2} - 15) + 3{h^*}^2(7\lambda^{12} - 9\lambda^8 + \lambda^6 - 9\lambda^2 + 10)\Big) - 3\beta\lambda^4 \widehat{D}_2^2] \tag{26}$$

Equalizing the expression (26) to zero and taking $\beta = 0.5$ and $h^* = 0.2$ the critical values for the stretch can be obtained from a plot $m\Omega_1^*$ vs λ for several values of $\widehat{D}_2$ (Figure 6) as follows

$$m\Omega_1^* = \frac{1.5\lambda^4\widehat{D}_2^2 - [(\lambda^6+5)+0.6(\lambda^8+\lambda^2)]}{\left[\begin{matrix}(6\lambda^8-3\lambda^6+3\lambda^2+9\lambda^{-4}-15)+0.2(15\lambda^{10}-9\lambda^8-3\lambda^6-9\lambda^2+21\lambda^{-2}-15)+\\ +0.12(7\lambda^{12}-9\lambda^8+\lambda^6-9\lambda^2+10)\end{matrix}\right]} \tag{27}$$

From Eq. (27) it is possible to estimate for values of $m\Omega_1^*$ and $\widehat{D_2}$ the stability limits in terms of the stretching λ . A comparison of the Figures (2) and (6) shows the differences between the two method used in the bifurcation analysis.

4. Ogden model.

The free energy of the model proposed by Ogden can be adequately represented by the following equation

$$\omega^*(\lambda_1,\lambda_2,\lambda_3) = \sum_{p=1}^{N}\frac{\mu_p}{\alpha_p}(\lambda_1^{\alpha_p}+\lambda_2^{\alpha_p}+\lambda_3^{\alpha_p}-3) \tag{28}$$

For equibiaxial deformations, taking N=3, and adding the electrostatic energy term one obtains:

$$\omega^*(\lambda,D_{L2}) = \sum_{p=1}^{3}\frac{\mu_p}{\alpha_p}(2\lambda^{\alpha_p}+\lambda^{-2\alpha_p}-3)+\frac{\beta}{2\varepsilon_0}\lambda^{-4}D_{L2}^2 \tag{29}$$

In order to be more specific the following values for α_p are adopted

$$\alpha_1 = 2, \alpha_2 = 4, \alpha_3 = -2 \tag{30}$$

from which the free energy reduces to

$$\omega^*(\lambda,D_{L2}) = \frac{\mu_1}{2}\left[(I_1-3)+\frac{h_1^*}{2}(I_1^2-2I_2-3)-h_2^*(I_2-3)+\frac{\beta}{\varepsilon_0\mu_1}\lambda^{-4}D_{L2}^2\right] \tag{31}$$

where $h_1^* = \frac{\mu_2}{\mu_1}, h_2^* = \frac{\mu_3}{\mu_1}$ and the definitions for the first and second invariants are taken into account.

By using Eq. (B14) the following expressions for the material parameters are obtained

$$a = 2\Omega_1^*\lambda^2+2\Omega_2^*\lambda^4; 2b = 2(\lambda^2+\lambda^{-4})(\Omega_1^*+\lambda^2\Omega_2^*)+4\Omega_{11}^*(\lambda^2-\lambda^{-4})^2+\frac{2\beta}{\varepsilon_0\mu_1}\lambda^{-4}D_{L2}^2; c = 2\Omega_1^*\lambda^{-4}+2\Omega_2^*\lambda^{-2}+\frac{2\beta}{\varepsilon_0\mu_1}\lambda^{-4}D_{L2}^2; d = \frac{2\beta}{\varepsilon_0}\lambda^{-2}D_{L2}; e = 2d; f = g = \frac{2\beta}{\varepsilon_0} \tag{32}$$

where $\Omega_1^* = \frac{\mu_1}{2}(1+h_1^*I_1); \Omega_2^* = -\frac{\mu_1}{2}(h_1^*+h_2^*); \Omega_{11}^* = \frac{\mu_1}{2}h_1^*; \Omega_5^* = \frac{\beta}{\varepsilon_0}$

the remaining terms being nil.

Dividing by $\frac{\mu_1}{2}$ and taking for simplicity $h_1^* = -h_2^* = h^*$, Eq. (B16) can be solved to give the following roots

$s_1 = -s_2 = 1$

$$s_3 = -s_4 = \frac{1}{2^{1/2}}\left\{\begin{matrix} \left(\lambda^6 + 1 + \frac{h^*(\lambda^4 - \lambda^{-2})^2}{1 + h^* I_1}\right) - \\ - \\ \left[\left(\lambda^6 + 1 + \frac{h^*(\lambda^4 - \lambda^{-2})^2}{1 + h^* I_1}\right)^2 - 4\lambda^6\right]^{\frac{1}{2}} \end{matrix}\right\}^{\frac{1}{2}}$$

$$s_5 = -s_6 = \frac{1}{2^{1/2}}\left\{\begin{matrix} \left(\lambda^6 + 1 + \frac{h^*(\lambda^4 - \lambda^{-2})^2}{1 + h^* I_1}\right) + \\ + \\ \left[\left(\lambda^6 + 1 + \frac{h^*(\lambda^4 - \lambda^{-2})^2}{1 + h^* I_1}\right)^2 - 4\lambda^6\right]^{\frac{1}{2}} \end{matrix}\right\}^{\frac{1}{2}} \qquad (33)$$

As above, in the absence of electric field the roots given by the Eq. (33) reduce to

$$s_1 = -s_2 = \frac{1}{2^{1/2}}\left\{\begin{matrix} \left(\lambda^6 + 1 + \frac{h^*(\lambda^4 - \lambda^{-2})^2}{1 + h^* I_1}\right) - \\ - \\ \left[\left(\lambda^6 + 1 + \frac{h^*(\lambda^4 - \lambda^{-2})^2}{1 + h^* I_1}\right)^2 - 4\lambda^6\right]^{\frac{1}{2}} \end{matrix}\right\}^{\frac{1}{2}}$$

$$s_3 = -s_4 = \frac{1}{2^{1/2}}\left\{\begin{matrix} \left(\lambda^6 + 1 + \frac{h^*(\lambda^4 - \lambda^{-2})^2}{1 + h^* I_1}\right) + \\ + \\ \left[\left(\lambda^6 + 1 + \frac{h^*(\lambda^4 - \lambda^{-2})^2}{1 + h^* I_1}\right)^2 - 4\lambda^6\right]^{\frac{1}{2}} \end{matrix}\right\}^{\frac{1}{2}} \qquad (34)$$

4.1. Results and Discussion.

In Figure 7, plots of λ_{cr} vs. kH for $h^* = 0.2$ and different values of the electric field are shown. The Figure 7a illustrates the case when the applied field is absent. A peak appears in the upper branch of the λ_{cr} vs. *kH* plots at about *kH=1* for $\widehat{D_2^2} > 1$. For values of the field higher than $\widehat{D_2^2} = 2.3$ two unstable regions appear in the bifurcation map, one for $\lambda_{cr} > 1$ and the other for $\lambda_{cr} < 1$. The first one broadens and tends to move to higher values of λ_{cr} with the electric field. On the contrary the second diminishes with the electric field as in the previous case. Clearly, the qualitative results of the analysis only are valid for the parameters given by Eq. (30). Further analysis for other parameters is now in progress.

4.2. Comparison with the Hessian approach.

In the present case the determinant of the matrix given by Eq. (25) leads to

$$\sum_{p=1}^{3}\mu_p\left[\left(\alpha_p-1\right)\lambda^{\alpha_p-2}+\left(2\alpha_p+1\right)\lambda^{-2\alpha_p-2}\right]-\frac{3\beta}{\varepsilon_0}\lambda^{-6}D_{L2}^2 \tag{35}$$

Eq. (35) with the chosen values for μ_p ,α_p and taking, as above, $h_1^*=-h_2^*=h^*$ together with some simplification leads to

$$\lambda^4(\lambda^6+5)+3h^*(2\lambda^{12}+\lambda^6+1)=3\beta\lambda^8\widehat{D_2^2} \tag{36}$$

As above, equalizing Eq. (36) to zero and taking $h^*=0.2$ and $\beta=0.5$ a plot of the critical stretch versus $\widehat{D_2}$ are obtained as Figure 8 which is close to the Figure 4b of [14]. The differences between the two methods of analysis can also be understood at the sight of the Figure (8). This figure shows that for $\widehat{D_2}<2.12$ no instability occurs. For $\widehat{D_2}>2.12$ the electric field has a destabilizing effect, and a lateral stretch needs to be applied in order to prevent instability.

Summing up, the Hessian approach is purely constitutive and does not account for the plate thickness, thus resulting in a very different stability criterion from that based in the incremental formulation.

5. Conclusions.

Two main conclusions can be obtained from the preceding analysis. First, it is noticeable the striking contrast between the results obtained by means of the two methodologies to analyze the stability, the so-called hessian by one side and the incremental by the other, a fact stressed in [14]. The second is the inherent limitations of the empirical models used to represent the actual behaviour of these materials. It is obvious that more complex models must be chosen to better represent the actual behaviour. However, this fact, introduce new parameters, mostly unknown at present and makes the formal treatment more complicated. Under these conditions.it is advisable that many new questions can arise concerning the instability and bifurcation phenomena in electroelastic materials which opens a suggestive field for future research.

Acknowledgements.

R.D.C. thanks to Professor Ogden the suggestions made in preparing this manuscript.

Funding.

This research did not receive any specific grant from funding agencies in the public, commercial, or not-for-profit sectors.

6. References.

1) X. Zhao,W. Hong,Z. Suo,. *Electromechanical hysteresis and coexistent states in dielectric elastomers*. Phys. Rev B 76,134113, (2007).
2) X. Zhao,Z. Suo, *Method to analyze electromechanical stability of dielectric elastomers,* Appl. Phys. Lett. 91,061921, (2007).
3) M. Moscardo,X. Zhao,Z. Suo,Y. Lapusta, *Analysis and manufacture of an energy harvester based on a Mooney-Rivlin–type dielectric elastomer*. J.Appl. Phys.104,093503, (2008).
4) R. Diaz-Calleja,M.J. Sanchis,E. Riande, *Effect of an electric field on the deformation of incompressible rubbers: Bifurcation phenomena*. J. of Electrostatics, 67,158-166, (2009).
5) R. Diaz-Calleja,M.J. Sanchis,E. Riande, *Effect of an electric field on the bifurcation of a biaxially stretched incompressible slab rubber*. Eur. Phys. J. E, 30,417-426, (2009).
6) J. Leng,L. Liu,Y. Liu,S. Sun, Appl. Phys. *Electromechanical stability of dielectric elastomer*. Lett.94,211901, (2009).
7) Y. Liu,L. Liu,S. Sung,J. Leng, *Electromechanical stability of a Mooney–Rivlin-type dielectric elastomer with nonlinear variable permittivity*. Pol. International, 59,371-377, (2010).
8) Z. Suo, *Theory of dielectric elastomers*. Acta Mechanica Solida Sinica, 23,549-578, (2010).
9) J. Zhu,H. Stoyanov,G. Kofod,Z. Suo, *Large deformation and electromechanical instability of a dielectric elastomer tube actuator*. J. Appl. Phys., 108,074113, (2010).
10) B.X. Xu,R. Mueller,M. Klassen,D. Gross, *On electromechanical stability analysis of dielectric elastomer actuators*. Appl. Phys. Lett. 97,162908,(2010).
11) X. Zhao,S.J.A. Koh,Z. Suo, *Nonequilibrium thermodynamics of dielectric elastomers*. Int. J. Appl. Mech.,3,203-217,(2011).
12) S.M.A. Jimenez,R.M. McMeeking, *Deformation dependent dielectric permittivity and its effect on actuator performance and stability*. Int. J. of Non-Linear Mechanics 57,183-191,(2013).
13) A. Dorfmann, R.W. Ogden, *Nonlinear electroelastostatics: Incremental equations and stability*. Int. J. of Engn. Sci. 48,1-14,(2010).
14) Luis Dorfmann, R.W. Ogden, *Instabilities of an electroelastic plate*. Int. J. of Engn. Sci. 77,79-101,(2014).

15) A. Dorfmann,R.W. Ogden, *Nonlinear electroelasticity*. Acta Mechanica 174,167-183, (2005).
16) A.E. Green,W. Zerna, *Theoretical Elasticity*, Oxford U.P. (1954).
17) I-Shih Liu *Continuum Mechanics*, p. 159, Springer-Verlag, Berlin, (2002).
18) R. W. Ogden, *Non-linear Elastic Deformations*, Dover, N. York, (1984).

Appendix A. The basic equations governing nonlinear electroelasticity.

Finite electroelasticity.

Let us consider a deformable electroelastic system that in the stress-free reference configuration is denoted by $\mathcal{B}_r$ with boundary $\partial\mathcal{B}_r$. After the application of the mechanical and electrical force fields the material will have the configuration $\mathcal{B}$ with boundary $\partial\mathcal{B}_r$. In the absence of mechanical body forces the equilibrium equation in Eulerian form leads to

$$div\boldsymbol{\tau} = \mathbf{0} \qquad \text{(A1)}$$

where $\boldsymbol{\tau}$ is the total Cauchy stress tensor satisfying the following boundary condition on any part of $\partial\mathcal{B}$

$$\boldsymbol{\tau}\boldsymbol{n} = \boldsymbol{t}_a \qquad \text{(A2)}$$

where $\mathbf{t}_a$ is the applied mechanical stress. Note that no Maxwell traction is assumed because the complient electrodes.

In absence of free charges inside the material the electromagnetic equations reduce to

$$div\boldsymbol{D}=0,\ \ curl\boldsymbol{E} = \mathbf{0} \qquad \text{(A3)}$$

In presence of a free charge σ_f per unit area of surface the boundary conditions are

$$\boldsymbol{n}\times\boldsymbol{E} = \mathbf{0}, \boldsymbol{n}\cdot\boldsymbol{D} = -\sigma_f \qquad \text{(A4)}$$

It is more convenient to work in terms of a Lagrangian formulation. Thus, if one denotes respectively by $\boldsymbol{X}$ and $\boldsymbol{x}$ the material points in the reference and in the deformed configurations which are related via the function $\boldsymbol{\chi}$, such that $\boldsymbol{x} = \boldsymbol{\chi}(\boldsymbol{X})$**.** The second-order tensor $\boldsymbol{F} = Grad\,\boldsymbol{\chi}$ is the deformation gradient referred to $\boldsymbol{X}$. The total nominal stress tensor $\boldsymbol{T}$ is defined by $\boldsymbol{T} = J\boldsymbol{F}^{-1}\boldsymbol{\tau}$, where $J = det\boldsymbol{F}$, satisfying the equilibrium equation.

$$Div\boldsymbol{T} = \mathbf{0} \qquad \text{(A5)}$$

In the case of incompressible materials, one has $J = 1$.

The corresponding boundary condition is

$$\boldsymbol{T}^T\boldsymbol{N} = \boldsymbol{t}_{\boldsymbol{A}} + \boldsymbol{T}_E^{\star T}\boldsymbol{N},\ \ \boldsymbol{T}_E^{\star} = J\boldsymbol{F}^{-1}\boldsymbol{\tau}_{\boldsymbol{e}}^{\star} \qquad \text{(A6)}$$

on $\partial\mathcal{B}_r$, where ^{T} means the transpose of a second-order tensor and $\mathbf{N}$ is the unit outward normal to $\partial\mathcal{B}_r$.

The (nominal) electric field $\boldsymbol{E}_L$ and electric displacement $\boldsymbol{D}_L$ are defined now as

$$\boldsymbol{E}_L = \boldsymbol{F}^T\boldsymbol{E},\ \ \boldsymbol{D}_L = J\boldsymbol{F}^{-1}\boldsymbol{D} \qquad \text{(A7)}$$

where the subscript L is referred to the Lagrangian formulation

These satisfy the following field equations

$$Div\,\boldsymbol{D}_L = 0,\ \ Curl\,\boldsymbol{E}_L = \mathbf{0} \qquad \text{(A8)}$$

where the capitals indicate that the vector operators are taken with respect to $\boldsymbol{X}$.

The corresponding boundary conditions in Lagrangian form are given by

$$\boldsymbol{N}\cdot\boldsymbol{D_L} = -\sigma_{\boldsymbol{F}},\ \ \boldsymbol{N}\times\boldsymbol{E}_L = \boldsymbol{0} \tag{A9}$$

where $\sigma_{\boldsymbol{F}}$ is the free charge density per unit area of $\partial\mathcal{B}_r$.

A total free energy density function $\Omega^*(\boldsymbol{F},\boldsymbol{D}_L)$ is assumed from which for such incompressible material ($\det\boldsymbol{F} = 1$).

$$T = \frac{\partial\Omega^*}{\partial\boldsymbol{F}} - p^*\boldsymbol{F}^{-1}, \boldsymbol{E}_L = \frac{\partial\Omega^*}{\partial\boldsymbol{D}_L}, \boldsymbol{\tau}=\boldsymbol{F}\frac{\partial\Omega^*}{\partial\boldsymbol{F}} - p^*\boldsymbol{I}, \boldsymbol{E} = \boldsymbol{F}^{-\boldsymbol{T}}\frac{\partial\Omega^*}{\partial\boldsymbol{D}_L} \tag{A10}$$

Where $p^*$is a Lagrange multiplier coming from the incompressibility condition.

Of course other definitions for the free energy function are possible as referred in Ref. [15].

For isotropic electroelastic materials $\Omega^*$is an isotropic function of the tensors $\boldsymbol{C} = \boldsymbol{F}^T\boldsymbol{F}$ and $\boldsymbol{D}_L\otimes\boldsymbol{D}_L$. In the case of incompressible materials the dependence of Ω^* is reduced to the following invariants

$$I_1 = Tr\boldsymbol{C},\ \ I_2 = \frac{\boldsymbol{1}}{\boldsymbol{2}}[(Tr\boldsymbol{C})^{\boldsymbol{2}} - (Tr\boldsymbol{C}^{\boldsymbol{2}})],\ \ I_4 = |\boldsymbol{D}_L^2|,\ \ I_5 = \boldsymbol{D}_L\cdot(\boldsymbol{C}\boldsymbol{D}_L),\ \ I_6 = \boldsymbol{D}_L\cdot(\boldsymbol{C}^2\boldsymbol{D}_L) \tag{A11}$$

where Tr is the trace of a second order tensor.

Then, one can set $\Omega^* = \Omega^*(I_1, I_2, I_4, I_5, I_6)$, and from the Eq. (A10) the total stress and the electric field are obtained in the Eulerian forms

$$\boldsymbol{\tau} = \boldsymbol{2}\Omega_1^*\boldsymbol{B} + \boldsymbol{2}\Omega_2^*(I_1\boldsymbol{B} - \boldsymbol{B}^2) - p^*\boldsymbol{I} - \boldsymbol{2}\Omega_5^*\boldsymbol{D}\otimes\boldsymbol{D} + \boldsymbol{2}\Omega_6^*[\boldsymbol{D}\otimes\boldsymbol{B}\boldsymbol{D} + \boldsymbol{B}\boldsymbol{D}\otimes\boldsymbol{D}]$$
$$\boldsymbol{E} = 2(\Omega_4^*\boldsymbol{B}^{-\boldsymbol{1}}\boldsymbol{D} + \Omega_5^*\boldsymbol{D} + \Omega_6^*\boldsymbol{B}\boldsymbol{D}) \tag{A12}$$

where Ω_i^* is defined as $\frac{\partial\Omega^*}{\partial I_i}$ for $i = 1,2,4,5,6$

The Lagrangian counterparts are obtained from $\boldsymbol{T} = \boldsymbol{F}^{-1}\boldsymbol{\tau},\ \ \boldsymbol{E_L} = \boldsymbol{F^T}\boldsymbol{E}$.

Appendix B. Incremental formulation.

Following the notation of Ref. [14], an increment in a variable will be represented by a superposed dot.

For the forthcoming analysis it is convenient to update the variables in such a way that $\mathcal{B}$ becomes the reference configuration. The resulting variables will be identified with a subscript 0 and, consequently, one has

$$\dot{\boldsymbol{E}}_{L0} = \boldsymbol{F}^{-T}\dot{\boldsymbol{E}}_L,\ \ \dot{\boldsymbol{D}}_{L0} = \boldsymbol{F}\dot{\boldsymbol{D}}_L,\ \ \dot{\boldsymbol{T}}_0 = \boldsymbol{F}\dot{\boldsymbol{T}} \tag{B1}$$

The incremental equations are updated to

$$div\,\dot{\boldsymbol{D}}_{L0} = 0,\ \ curl\,\dot{\boldsymbol{E}}_{L0} = \boldsymbol{0},\ div\,\dot{\boldsymbol{T}}_0 = \boldsymbol{0} \tag{B2}$$

and, after the pertinent calculations, the following incremental forms of the traction and electrical boundary conditions for incompressible materials now on $\partial\mathcal{B}$ lead to

$$\dot{\boldsymbol{T}}_0^T\boldsymbol{n} = \dot{\boldsymbol{t}}_{A0} \quad on \ \ \partial\mathcal{B}$$
$$\dot{\boldsymbol{D}}_{L0}\cdot\boldsymbol{n} = -\dot{\sigma}_{F0} \quad on \ \ \partial\mathcal{B} \tag{B3}$$
$$\dot{\boldsymbol{E}}_{L0}\times\boldsymbol{n} = \boldsymbol{0} \quad on \ \ \partial\mathcal{B}$$

where $\dot{\sigma}_{F0} = \dot{\sigma}_F \frac{dA}{da}$ is the increment of free surface charge. The incremental incompressibility condition leads to

$$div\mathbf{u} = 0 \tag{B4}$$

Let us consider now an incremental deformation $\dot{\boldsymbol{F}}$ superimposed to an increment in the Lagrangian electric field $\dot{\boldsymbol{D}}_L$ in the configuration $\mathcal{B}$. Then, the linear incremental expressions for $\dot{\boldsymbol{T}}_0$ and $\dot{\boldsymbol{E}}_{L0}$ for an unconstrained and incompressible material in the Eulerian form, are [14]

$$\dot{\boldsymbol{T}}_0 = \boldsymbol{\mathcal{A}}_0^*\boldsymbol{L} + \mathbb{A}\dot{\boldsymbol{D}}_{L0} + p^*\boldsymbol{L} - \dot{p}^*\boldsymbol{I}, \ \ \dot{\boldsymbol{E}}_{L0} = \mathbb{A}_{\boldsymbol{0}}^{*T}\boldsymbol{L} + \boldsymbol{A}_{\boldsymbol{0}}^*\dot{\boldsymbol{D}}_{L0} \tag{B5}$$

where $\boldsymbol{L} = grad\ \boldsymbol{u}$ and $\boldsymbol{\mathcal{A}}_0^*, \mathbb{A}_0^*, \boldsymbol{A}_0^*$ are, respectively, the fourth-,third- and second-order electroelastic moduli tensors associated with the total energy $\Omega^*(\boldsymbol{F}, \boldsymbol{D}_L)$.

These can be writen in component form for incompressible materials as

$$\mathcal{A}_{0jikl}^* = F_{j\alpha}F_{l\beta}\frac{\partial^2\Omega^*}{\partial F_{i\alpha}\partial F_{j\beta}}, \ \ \mathbb{A}_{0\alpha i|\beta}^* = \frac{\partial^2\Omega^*}{\partial F_{i\alpha}\partial D_{L\beta}}, \ \ A_{\alpha\beta}^* = \frac{\partial^2\Omega^*}{\partial D_{L\alpha}\partial D_{L\beta}} \tag{B6}$$

The vertical bar between the indices in the second equation (B6), is used to distinguish the single subscript from the pair of subscripts going together. The following symmetry conditions for these tensors are fulfilled [15]

$$\mathcal{A}_{0\alpha i\beta j}^* = \mathcal{A}_{0\beta j\alpha i}^*, \ \ \mathbb{A}_{0ij|k}^* = \mathbb{A}_{0ji|k}^*, \ \ A_{0\alpha\beta}^* = A_{0\beta\alpha}^* \tag{B7}$$

It is to be noted that for an unconstrained electroelastic material Ω^* is a function of the six invariants $I_1, \ldots, I_6$ and Eq. (B 6) can be expanded in terms of the first and second order derivatives of the invariants (e.g. Eq. (28) of Ref. [13]).

The next step is to specialize the incremental formulation derived in Appendix B for the specific geometry of our problem. For this purpose, taking into account that the deformation is equibiaxial the incremental displacement will be a plane strain in the (x_1, x_2) plane. The incremental displacement vector will be $\boldsymbol{u} = (u_1, u_2, 0)$ which only depend on x_1 and x_2. Thus, the incompressibility condition reduces to

$$u_{1,1} + u_{2,2} = 0 \tag{B8}$$

where as usual a comma in the subscript indicates partial differentiation with respect the corresponding variable.

In analogy, one defines $\dot{\boldsymbol{D}}_{L0} = (\dot{D}_{L01}, \dot{D}_{L02}, 0)$ with components that depend only on x_1 and x_2.These components must satisfy the first equation of (B2), that is

$$\dot{D}_{L01,1} + \dot{D}_{L02,2} = 0 \tag{B9}$$

Eq. (B8, B9) predict the existence of functions $\psi = \psi(x_1, x_2)$ and $\varphi = \varphi(x_1, x_2)$ in such a way that

$$u_1 = \psi_{,2},\ \ u_2 = -\psi_{,1} \text{ and } \dot{D}_{L01} = \varphi_{,2},\ \ \dot{D}_{L02} = -\varphi_{,1} \tag{B10}$$

and $\varphi_{,11} + \varphi_{,22} = 0$ according to the Laplace equation.

From the third and the second equations in (B2), one obtains

$$\dot{T}_{011,1} + \dot{T}_{021,2} = 0,\ \ \dot{T}_{012,1} + \dot{T}_{022,2}\ ,\dot{E}_{L01,2} - \dot{E}_{L02,1} = 0 \tag{B11}$$

where the components of $\dot{\boldsymbol{T}}_{\mathbf{0}}$ and $\dot{\boldsymbol{E}}_{L0}$ are obtained from Eq. (B5).

After the pertinent calculations, the updated incremental total nominal stress tensor and the Lagrangian electric displacement non-zero components can be easily calculated. The results as well as the incremental boundary conditions in terms of the functions ψ and φ are

$$(\mathcal{A}^*_{01111} - \mathcal{A}^*_{01221} - \mathcal{A}^*_{01122})\psi_{,112} + \mathcal{A}^*_{02121}\psi_{,222} - \mathbb{A}^*_{011|2}\varphi_{,11} + \mathbb{A}^*_{021|1}\varphi_{223} = \dot{p}^*_{,1}$$
$$(\mathcal{A}^*_{02222} - \mathcal{A}^*_{01122} - \mathcal{A}^*_{01221})\psi_{,122} + \mathcal{A}^*_{01212}\psi_{,111} - (\mathbb{A}^*_{012|1} - \mathbb{A}^*_{022|2})\varphi_{,12} = -\dot{p}^*_{,2}$$
$$\left(\mathbb{A}^*_{021|1+} + \mathbb{A}^*_{011|2} - \mathbb{A}^*_{022|2}\right)\psi_{,122} - \mathbb{A}^*_{021|1}\psi_{,111} + (A_{011} - A_{022})\varphi_{,12} = 0$$

(B12)

After elimination of $\dot{p}^*$ from the first two of these equations, one obtains a system of equations for ψ and φ which may be written in compact form as

$$a\psi_{,1111} + 2b\psi_{,1122} + c\psi_{,2222} + (e-d)\varphi_{,112} + d\varphi_{,222} = 0$$
$$(e-d)\psi_{,122} + d\psi_{,111} - (f-g)\varphi_{,12} = 0$$

(B13)

where

$$a = \mathcal{A}^*_{01212},\ \ 2b = \mathcal{A}^*_{01111} + \mathcal{A}^*_{02222} - 2\mathcal{A}^*_{01221} - 2\mathcal{A}^*_{01122}, \qquad c = \mathcal{A}^*_{02121}$$
$$d = \mathbb{A}^*_{021|1},\ \ e = \mathbb{A}^*_{022|2} - \mathbb{A}^*_{011|2},\ \ f = A_{011},\ \ g = A_{022}$$

(B14)

are material parameters.

Small-amplitude solutions have been chosen, among others, to solve the incremental boundary-value problem as in Ref. [14].

$$\psi = A\exp(-ksx_2)\exp(ikx_1),\ \ \varphi = kB\exp(-ksx_2)\exp(ikx_1) \tag{B15}$$

where s is to be determined and k is the wave-number of the signals.

Substitution of (B15) in (B13) and subsequent check for non-trivial solutions of the homogeneous system resulting leads to the following cubic equation in s^2

$$(cf-d^2)s^6-[2bf+cg+2(d-e)]s^4+[2bg+af-(d-e)^2]s^2-ag=0 \tag{B16}$$

The general solution for the plate may be written as $A_j\exp(-ks_jx_3)\exp(ikx_1)$

$$\psi=\sum_{j=1}^{6}A_j\exp(-ks_jx_2)\exp(ikx_1),\ \ \varphi=k\sum_{j=1}^{6}B_j\exp(-ks_jx_2)\exp(ikx_1) \tag{B17}$$

The twelve unknown constants $A_j, B_j, j=1,\dots,6$ are not independent but they are related through the following equation

$$s_j(ds_j^2+d-e)A_j-(fs_j^2-g)B_j=0 \tag{B18}$$

For the configuration of compliant electrodes proposed in the Paragraph 2, remembering that there is no electric field outside the plate and assuming that neither applied nor incremental mechanical tractions are present, the incremental boundary conditions are

$$c(\psi_{,22}-\psi_{,11})+d\varphi_{,2}=0$$

$$on\ x_2=0,h$$

$$(2b+c)\psi_{,112}+c\psi_{,222}+e\varphi_{,11}+d\varphi_{,22}=0 \tag{B19}$$

The incremental electric boundary conditions reduce to

$$\dot{E}_{L01}=0,\ \ \dot{D}_{L02}=-\dot{\sigma}_{F0}\ on\ x_2=0,h \tag{B20}$$

which, after rewritten in terms of ψ,φ reduce to

$$d(\psi_{,22}-\psi_{,11})+f\varphi_{,2},\ \ \varphi_{,1}=\dot{\sigma}_{F0}\quad on\quad x_2=0,h \tag{B21}$$

Note that the field D_3 satisfy the jump condition $D_2=\sigma_f$ on $x_2=0,h$.

Substitution of (B17) in (B18), (B19) and (B21)$_1$ on the faces $x_2=0,h$, one obtains

$$\sum_{j=1}^{6}\left[c(1+s_j^2)A_j-ds_jB_j\right]=0$$

$$\sum_{j=1}^{6}\left[(2b+c-cs_j^2)s_jA_j-(e-ds_j^2)B_j\right]=0$$

$$\sum_{j=1}^{6}\left[d(1+s_j^2)A_j-fs_jB_j\right]=0$$

$$\sum_{j=1}^{6}\left[c(1+s_j^2)A_j-ds_jB_j\right]exp(-khs_j)=0$$

$$\sum_{j=1}^{6}\left[(2b+c-cs_j^2)s_jA_j-(e-ds_j^2)B_j\right]exp(-khs_j)=0$$

$$\sum_{j=1}^{6}\left[d\left(1+s_j^2\right)A_j - f s_j B_j\right]\exp(-khs_j) = 0 \tag{B22}$$

Eq. (B18) and (B22) form a homogeneous system of twelve linear equations for twelve unknowns. Non-trivial solutions are possible if the determinant of the coefficients of this system vanish. However, the size of the 12x12 determinant can be reduced to a 6x6 one by taking into account the relation between A_j and B_j.

Complex bifurcation maps in electroelastic elastomeric plates.

R. Díaz-Calleja, P. Llovera-Segovia, A. Quijano-López.

ITE, Universitat Politècnica de València, Cº Vera s/n, E-46022, Valencia (Spain)-Instituto Tecnológico de la Energía-Redit.

Abstract.

Stress-strain relationships for rubbery materials are highly non-linear. In this work, a particular configuration of electroactive material is considered: an isotropic, incompressible electroelastic squared plate is subjected to equal biaxial homogeneous deformation and a scalar electrical potential is applied on the sides of compliant electrodes. This case is analysed according to two methodologies: the Hessian approach and the use of incremental deformation together with increment in the electric displacement. First, an extended Mooney-Rivlin model is considered for the material and then an Ogden model is also analysed. Results, show, that despite of available experimental results, some predictions can be made and the pertinent analysis show complex bifurcation maps. This can help in the future progress in the knowledge of the instabilities and bifurcation phenomena which should appear in these materials. The present paper has been mainly motivated by the work of Ogden and Dorfmann.

1. Introduction.

Stress-strain relationships for rubbery materials are highly non-linear. As a consequence, solutions of many traction boundary problems are not unique. Concomitantly, due to the nonconvexity of the free energy function, instability and bifurcation phenomena appear giving rise to problems in the design of sensor and actuators devices. For this reason, the analysis of these phenomena in these electroactive elastomers is compulsory in order to have a better understanding of the actual behaviour of these materials and avoid undesirable unstable behaviour.

Instabilities in thin plates of electroelastic materials have been theoretically predicted by using homogeneous deformations and regardless of the thickness of the plates. The Hessian approach has been used in the current literature to analyse these instabilities [1-12]. By contrast, the use of incremental deformation together with increment in the electric displacement has revealed to be a more powerful tool to analyse the case where non-homogeneous deformations and plate thickness are considered [13, 14]. In these circumstances the inherent formal treatment requires, in general, new material parameters implying a more complex analysis. However, due to the scarcity of experimental knowledge of these parameters, a detailed characterization of the unstable behaviour of these electroactive elastomers is not possible at present.

In spite of that, some predictions can be made in some particular cases and the pertinent analysis show complex bifurcation maps. This can help in the future progress in the knowledge of the instabilities and bifurcation phenomena which should appear in these materials. The present paper has been mainly motivated by the work of Ogden and Dorfmann [13, 14, 15] which is briefly summarized in Appendix A. In fact, the main target of the present study is to extend the study of the instability and bifurcation made in Ref. [13, 14] by applying more realistic electroelastic models than the neo-Hookean one. In the pertinent analysis of the problem new facts appear that merit consideration.

2. Geometry, finite deformation and incremental formulation.

Thus, in the spirit of Dorfmann and Ogden [14], an isotropic, incompressible electroelastic squared plate is subjected to equal biaxial homogeneous deformation and a scalar electrical potential is applied on the sides of compliant electrodes. Specifically, let us assume a plate of initial thickness H subjected to a plane strain biaxial stretch in the directions 1, 3 and a normal electric force field in the direction 2. The plate will be considered to be bounded by flexible (compliant) electrodes. Thus, it will be assumed that no electric field exists outside the plate (see App. A). The continuity condition applied to the boundary $x_2 = h$ (being h the actual thickness of the plate) under incompressibility condition gives $D_{L2} = -\sigma_F$. where D_{L2} is the Lagrangian component of the electric displacement (see Eq. A7).

In the general case, if $\lambda_1, \lambda_2, \lambda_3$ are the principal stretches, the invariants are

$$I_1 = \lambda_1^2 + \lambda_3^2 + \lambda_1^{-2}\lambda_3^{-2}, \;\; I_2 = \lambda_1^{-2} + \lambda_3^{-2} + \lambda_1^2\lambda_3^2,$$

$$I_4 = D_{L2}^2, I_5 = \lambda_1^{-2}\lambda_3^{-2}D_{L2}^2, \;\; I_6 = \lambda_1^{-4}\lambda_3^{-4}D_{L2}^2 \qquad (1)$$

In this case, the principal stresses and the electric field are

$$\tau_{11} = \lambda_1 \frac{\partial \Omega^*}{\partial \lambda_1} - p^*$$

$$\tau_{33} = \lambda_3 \frac{\partial \Omega^*}{\partial \lambda_2} - p^*$$

$$\tau_{22} = \lambda_2 \frac{\partial \Omega^*}{\partial \lambda_3} - p^* + 2\Omega_5^* \lambda_1^{-2} \lambda_3^{-2} D_{L2}^2 + 4\Omega_6^* \lambda_1^{-4} \lambda_3^{-4} D_{L2}^2$$

$$E_2 = E_{L2} \lambda_2^{-1} = 2(\Omega_4^* \lambda_2^{-1} + \Omega_5^* \lambda_2 + \Omega_6^* \lambda_2^3) D_{L2} \qquad (2)$$

where p^* is a Lagrange multiplier becoming from the incompressibility condition and Ω^* is the free energy density and Ω_i^* is defined as $\frac{\partial \Omega^*}{\partial I_i}$ for $i = 1,2,4,5,6$.

The elimination of p^*leads to

$$\tau_{11} - \tau_{22} = \lambda_1 \frac{\partial \widehat{\Omega}^*}{\partial \lambda_1} - 2\widehat{\Omega}_5^* \lambda_1^{-2} \lambda_3^{-2} D_{L2}^2 - 4\widehat{\Omega}_6^* \lambda_1^{-4} \lambda_3^{-4} D_{L2}^2$$

$$\tau_{33} - \tau_{22} = \lambda_3 \frac{\partial \widehat{\Omega}^*}{\partial \lambda_3} - 2\widehat{\Omega}_5^* \lambda_1^{-2} \lambda_3^{-2} D_{L2}^2 - 4\widehat{\Omega}_6^* \lambda_1^{-4} \lambda_3^{-4} D_{L2}^2 \qquad (3)$$

where the free energy has been redefined as $\widehat{\Omega}^*(\lambda_1, \lambda_3, I_4, I_5, I_6)$.

For the incompressibility condition and Eq. (1), only three independent variables remain.

Thus, let us take these to be $\lambda_1, \lambda_3, D_{L2}$ and define $\widetilde{\Omega}^*$ where $\widetilde{\Omega}^*(\lambda_1, \lambda_3, D_{L2}) = \widehat{\Omega}^*(\lambda_1, \lambda_3, I_4, \lambda_2^2 I_4, \lambda_2^4 I_4)$ is a new reduced form of the free energy density taken into account that only three independent variables $\lambda_1, \lambda_3, D_{L2}$ remain in the problem.

Now, it is assumed that the plate is bounded by flexible (compliant) electrodes on $x_2 = 0, h$ and free surface charges $-\sigma_f, \sigma_f$ per unit area are placed, respectively, on each electrode.

If no traction exists on the faces then $\tau_{22} = 0$ and two first equations of (3) simplify to

$$\lambda_1 T_{11} = \tau_{11} = \lambda_1 \frac{\partial \widetilde{\Omega}^*}{\partial \lambda_1}, \quad \lambda_3 T_{33} = \tau_{33} = \lambda_3 \frac{\partial \widetilde{\Omega}^*}{\partial \lambda_3}, \qquad (4)$$

and $E_2 = \lambda_2^{-1} \frac{\partial \widetilde{\Omega}^*}{\partial D_{L2}}$.

where T_{11} and T_{33} are the nominal stress components.

If the potential difference between the electrodes is V and the electric field is uniform then $V = E_2 h = E_{L2} H$ and $h = \lambda_1 \lambda_3 H$.

For equibiaxial deformations $\lambda_1 = \lambda_3 = \lambda$, which implies $\lambda_2 = \lambda^{-2}$, one can define a reduced form of the energy function $\omega^* = \omega^*(\lambda, D_{L2})$. In this case, the two non-zero components of the stress are $\tau_{11} = \tau_{33} = \tau$, where

$$\tau = \frac{1}{2} \lambda \frac{\partial \omega^*}{\partial \lambda} = 2(\Omega_1^* + \lambda^2 \Omega_2^*)(\lambda^2 - \lambda^{-4}) - 2\Omega_5^* D_2^2 - 4\Omega_6^* \lambda^{-4} D_2^2 \qquad (5)$$

and Ω_i^* denotes the derivative of the free energy with respect to I_i and $D_2 = \lambda^{-2} D_{L2}$ relating the Eulerian and Lagrangian electric displacement.

From the preceding equations an analysis of the stability can be outlined as in Ref. [1-12]. However, to fully analyze the stability of electroelastic plates the possibility of non-homogeneous deformations and the dependence on the plate thickness can´t be ruled out. Consequently, in the remaining part of the paper an incremental strategy has been outlined as in Ref. [14]. The basic idea underlying the incremental formulation is to use small deformations and electric displacements superimposed on a known large deformation [16]. The pertinent details are summarized in Appendix B.

3. Extended Mooney-Rivlin model.

In order to consider a more general model than the neo-Hookean one, let us assume the following expression for the free energy that generalizes Eq. (5)

$$\omega^*(\lambda, m, D_{L2}) = \Omega_1^*\left[((I_1-3)+(I_2-3)h^*)+\frac{1}{2}m\Omega_1^*((I_1-3)+(I_2-3)h^*)^2+\frac{1}{2\epsilon_0\Omega_1^*}\beta\lambda^{-4}D_{L2}^2\right] \quad (6)$$

where $h^* = \Omega_2^*/\Omega_1^*$ and $I_1 = 2\lambda^2+\lambda^{-4}$, $I_2 = 2\lambda^{-2}+\lambda^4$

In eq. (6), m is a parameter affecting the second order term of the expansion in powers of the Mooney-Rivlin free energy density$(\Omega_1^*(I_1-3)+\Omega_2^*(I_2-3))$. In fact this equation generalizes the electroactive Mooney-Rivlin equation to include quadratic terms in the mechanical invariants. This generalization is, of course, a possible one among many others and has been chosen for illustrative purposes. The parameter is defined from Eq. (5) as $\beta = 2\Omega_5^*$. Eq. (6) implies that the permittivity is deformation independent and in this case β^{-1} can be interpreted as the relative permittivity. Concomitantly, the invariant I_6 is excluded in the proposed constitutive model. Moreover, if one makes $h^* = 0$ in Eq. (6), then the resulting constitutive equation is similar to the so-called equation for an "ideal dielectric elastomer" by Zhao and Suo [2].

Since no traction is present on the faces, $\tau_{22} = 0$ and from Eq. (5), the lateral stress is given by

$$\tau = 2\Omega_1^*\{[(\lambda^2-\lambda^{-4})(1+h^*\lambda^2)(1+m\Omega_1^*((I_1-3)+(I_2-3)h^*))]-\beta\widehat{D}_2^2\} \quad (7)$$

where $\widehat{D}_2 = \frac{D_2}{(2\Omega_1^*\varepsilon_0)^{\frac{1}{2}}}$

If no lateral traction is present, Eq. (7) leads to

$$\widehat{D}_2^2 = \beta^{-1}[(\lambda^2-\lambda^{-4})(1+h^*\lambda^2)(1+m\Omega_1^*((I_1-3)+(I_2-3)h^*))] \quad (8)$$

Since Ω_1^* and h^* and the relative permittivity are currently positive, if $m > 0$ the plate becomes thinner when the electric field increases.

Incremental equations include expressions for the tensors $\boldsymbol{\mathcal{A}}_{\mathbf{0}}^*, \mathbb{A}_{\mathbf{0}}^*, \boldsymbol{A}$ in terms of the first and second order derivatives of Ω^* with respect to the invariants (see App. B). Then, the material parameters given by Eq. (B14) for our incompressible material under biaxial stretching can be calculated by means of the Eq. (40-51) of Ref. [13].

Results are

$$a = 2\Omega_1^*\lambda^2(1 + h^*\lambda^2)(1 + m\Omega_1^*((I_1 - 3) + (I_2 - 3)h^*))$$

$$2b = 2\Omega_1^*[(\lambda^2 + \lambda^{-4})(1 + h^*\lambda^2)(1 + m\Omega_1^*((I_1 - 3) + (I_2 - 3)h^*))] + 4m{\Omega_1^*}^2(1 + h^*\lambda^2)^2(\lambda^2 - \lambda^{-4})^2 + 2\varepsilon_0^{-1}\beta D_2^2$$

$$c = 2\Omega_1^*\lambda^{-4}(1 + h^*\lambda^2)(1 + m\Omega_1^*((I_1 - 3) + (I_2 - 3)h^*)) + 2\varepsilon_0^{-1}\beta D_2^2$$

$$d = 2\varepsilon_0^{-1}\beta D_2$$

$$e = 4\varepsilon_0^{-1}\beta D_2$$

$$f = g = 2\varepsilon_0^{-1}\beta \qquad (9)$$

Then, the bi-cubic equation (B16) can be solved to give

$$s_1 = -s_2 = 1$$

$$s_3 = -s_4 = \frac{1}{2^{1/2}}\left\{\left(\lambda^6 + 1 + \frac{2m\lambda^{-4}(\lambda^6 - 1)^2(1 + h^*\lambda^2)}{1 + m\Omega_1^*((I_1 - 3) + (I_2 - 3)h^*)}\right) - \left[\left(\lambda^6 + 1 + \frac{2m\lambda^{-4}(\lambda^6 - 1)^2(1 + h^*\lambda^2)}{1 + m\Omega_1^*((I_1 - 3) + (I_2 - 3)h^*)}\right)^2 - 4\lambda^6\right]^{\frac{1}{2}}\right\}^{\frac{1}{2}}$$

$$s_5 = -s_6 = \frac{1}{2^{1/2}}\left\{\left(\lambda^6 + 1 + \frac{2m\lambda^{-4}(\lambda^6 - 1)^2(1 + h^*\lambda^2)}{1 + m\Omega_1^*((I_1 - 3) + (I_2 - 3)h^*)}\right) + \left[\left(\lambda^6 + 1 + \frac{2m\lambda^{-4}(\lambda^6 - 1)^2(1 + h^*\lambda^2)}{1 + m\Omega_1^*((I_1 - 3) + (I_2 - 3)h^*)}\right)^2 - 4\lambda^6\right]^{\frac{1}{2}}\right\}^{\frac{1}{2}}$$

(10)

Note that in these equations the electric displacement is absent. This is a consequence of the hypothesis $\alpha = 0$. In the case where $\alpha \neq 0$ no solutions $s_1 = -s_2 = 1$ of Eq. (16) appear what makes much more involved the solution of the present problem.

In the following developments the dimensionless variable

$$\hat{B}_j = \frac{B_j}{(2\Omega_1^*\varepsilon_0)^{\frac{1}{2}}} \qquad (11)$$

is introduced.

Substitution of Eq. (10, 11) in Eq. (B22), leads to

$$\sum_{j=1}^{6}\left[(\lambda^{-4}(1+h^*\lambda^2)(1+m\Omega_1^*((I_1-3)+(I_2-3)h^*))+\widehat{D}_2^2)\left(1+s_j^2\right)A_j-\widehat{D}_2 s_j\hat{B}_j\right]=0$$

$$\sum_{j=1}^{6}\{[(\lambda^2+2\lambda^{-4})(1+h^*\lambda^2)(1+m\Omega_1^*((I_1-3)+(I_2-3)h^*))+2m\Omega_1^*\lambda^4(1+h^*\lambda^2)^2(1-\lambda^{-6})^2+\widehat{D}_2^2-[\lambda^{-4}(1+h^*\lambda^2)(1+m\Omega_1^*((I_1-3)+(I_2-3)h^*))+\widehat{D}_2^2]s_j^2]s_jA_j-\widehat{D}_2(2-s_j^2)\hat{B}_j]\}=0$$

$$\sum_1^6\left[\widehat{D}_2\left(1+s_j^2\right)A_j-s_j\hat{B}_j\right]=0$$

$$\sum_{j=1}^{6}\left[(\lambda^{-4}(1+h^*\lambda^2)(1+m\Omega_1^*((I_1-3)+(I_2-3)h^*))+\widehat{D}_2^2)\left(1+s_j^2\right)A_j-\widehat{D}_2 s_j\hat{B}_j\right]e^{-ks_jh}=0$$

$$\sum_{j=1}^{6}\{[(\lambda^2+2\lambda^{-4})(1+h^*\lambda^2)(1+m\Omega_1^*((I_1-3)+(I_2-3)h^*))+2m\Omega_1^*\lambda^4(1+h^*\lambda^2)^2(1-\lambda^{-6})^2+\widehat{D}_2^2-[\lambda^{-4}(1+h^*\lambda^2)(1+m\Omega_1^*((I_1-3)+(I_2-3)h^*))+\widehat{D}_2^2]s_j^2]s_jA_j-\widehat{D}_2(2-s_j^2)\hat{B}_j]\}e^{-ks_jh}=0$$

$$\sum_1^6\left[\widehat{D}_2\left(1+s_j^2\right)A_j-s_j\hat{B}_j\right]e^{-ks_jh}=0 \qquad (12)$$

where in the biaxial stretching case $h=\lambda^{-2}H$ and A_j and $\hat{B}_j$ are defined in Eq. (B17). .

In the same way, Eq. (B18) leads to the following relationship between A_j and $\hat{B}_j$

$$(s_j^2-1)(s_j\widehat{D}_2A_j-\hat{B}_j)=0 \qquad (13)$$

Thus, if in (13) $s_j=\pm1, \hat{B}_j\neq s_j\widehat{D}_2A_j$ (in general)

$$s_j\neq\pm1, \hat{B}_j=s_j\widehat{D}_2A_j \qquad (14)$$

Incidentally, note that if one takes $m=0$ the equation (13) reduces to

$$(s^2-1)^2(s^2-\lambda^6)=0 \qquad (15)$$

and one returns to the extended Mooney-Rivlin model.

Eq. (13) and (14) indicate that only when $s_j, j=3,\dots,6$ there exists a connection between A_j and $\hat{B}_j$ whereas for $s_j, j=1,2$ such relation is undetermined and consequently the system of six homogeneous equations (12) has eight unknowns $A_j, j=1,\dots,6, \hat{B}_{j,}\ j=1,2$. It can be shown that if one assumes $\hat{B}_j=s_j\widehat{D}_2A_j$ for $j=1,2$ then the bifurcation map is independent of the applied electric field that seems an inconsistent result. For this reason it will be taken $\hat{B}_j=0,\ j=1,2$. This implies to modify the proposed solution for φ (cf. Eq. $(B17)_2$), that is,

$$\varphi=k\sum_{j=3}^{6}B_j\exp\left(-ks_jx_2\right)\exp(ikx_1) \qquad (16)$$

With these premises, the homogeneous system (12) results in a system of 6 equations with 6 unknowns and the corresponding determinant must vanish as usual for a non trivial solution.

This determinant is equalized to zero in order to identify the critical pre-stretch values $\lambda_{crit.}$ announcing the unstable behavior.

It is noticeable that the parameter *m* in Eq. (6) could be either positive or negative, for, respectively positive or negative deviations of the Mooney-Rivlin mechanical behaviour. As mentioned above, if *m* is positive, the function represented by Eq. (8) is increasing with λ and the plate thins with increasing the applied electric force field. However, if *m* is negative the situation is more complex. In order to compare the results with those of Ref. [14] one will take in the calculations that follow $\beta = 0.5$. Accordingly, in Figure 1 a plot of $\widehat{D}_2$ vs. λ for $\beta = 0.5$ and different values of $m\Omega_1^*$is shown. This plot indicates that for decreasing values of $m\Omega_1^*$ the plate tends to be more unstable and determines the limits of stability for the system under study. For this reason, only small negative values for $m\Omega_1^*$ seems to be physically reasonable. In order to be more specific in Figure 2 values of $m\Omega_1^*$ vs. λ for the chosen $\beta = 0.5$ and different applied electric fields are shown.

In absence of electric field, and according to the Eq. (9) and (B24), one obtains

$$s_1 = -s_2 = \frac{1}{2^{1/2}}\left\{\begin{array}{c}\left(\lambda^6 + 1 + \frac{2m\lambda^{-4}\left(\lambda^6-1\right)^2\left(1+h^*\lambda^2\right)}{1+m\Omega_1^*((I_1-3)+(I_2-3)h^*)}\right) \\ - \\ \left[\left(\lambda^6 + 1 + \frac{2m\lambda^{-4}\left(\lambda^6-1\right)^2\left(1+h^*\lambda^2\right)}{1+m\Omega_1^*((I_1-3)+(I_2-3)h^*)}\right)^2 - 4\lambda^6\right]^{\frac{1}{2}}\end{array}\right\}^{\frac{1}{2}}$$

$$s_3 = -s_4 = \frac{1}{2^{1/2}}\left\{\begin{array}{c}\left(\lambda^6 + 1 + \frac{2m\lambda^{-4}\left(\lambda^6-1\right)^2\left(1+h^*\lambda^2\right)}{1+m\Omega_1^*((I_1-3)+(I_2-3)h^*)}\right) \\ + \\ \left[\left(\lambda^6 + 1 + \frac{2m\lambda^{-4}\left(\lambda^6-1\right)^2\left(1+h^*\lambda^2\right)}{1+m\Omega_1^*((I_1-3)+(I_2-3)h^*)}\right)^2 - 4\lambda^6\right]^{\frac{1}{2}}\end{array}\right\}^{\frac{1}{2}} \quad (17)$$

which are the four roots differing of $s_{1,2} = \pm 1$ in Eq. (10).

Also note that in the absence of electric force field the bicubic equation [B16] reduces to a bicuadratic one and, in this case, one has

$$cs^4 - 2bs^2 + a = 0 \quad (18)$$

where *a*,*b*,*c* are given by

$$a = 2\Omega_1^*\lambda^2(1 + h^*\lambda^2)(1 + m\Omega_1^*((I_1 - 3) + (I_2 - 3)h^*))$$

$$b = \Omega_1^*[(\lambda^2 + \lambda^{-4})(1 + h^*\lambda^2)(1 + m\Omega_1^*((I_1 - 3) + (I_2 - 3)h^*))] + 4m{\Omega_1^*}^2(1 + h^*\lambda^2)^2(\lambda^2 - \lambda^{-4})^2$$

$$c = 2\Omega_1^*\lambda^{-4}(1 + h^*\lambda^2)(1 + m\Omega_1^*((I_1 - 3) + (I_2 - 3)h^*)) \quad (19)$$

The solutions of Eq. (18) are

$$s = \pm\left[\frac{b \pm (b^2 - ac)^{1/2}}{c}\right]^{1/2} \tag{20}$$

Then, on account of the relationship between A_j and B_j $(14)_1$ the problem reduces to examine the determinant of a 4x4 matrix corresponding to a system of four homogeneous equations with four unknowns.

3.1. Results and discussion.

In Figure 3, plots of $\lambda_{cr.}$ vs. *kH* with $m\Omega_1^* = 0.01$ and $h^* = 0.2$ for different values of the applied electric field are shown. The characteristic curves corresponding to the different modes of deformation tend to merge together for large values of *kH* and these values increase with the electric field. Moreover an upper branch that increases with *kH* appears. Figure 3a illustrates the case where the applied electric field is absent. In this particular case, the limiting value for $kH \to \infty$ is $\lambda_{cr.} \cong 0.6661$.

In general, for moderate electric fields, the plate becomes unstable for values of the lateral stretch below the upper curve but above the lower one. Thus, in order to prevent a loss of stability, the lateral stretch should be increased as the electric field increases. However, for larger electric fields the situation becomes more complex and, for example, the bifurcation map for $\widehat{D}_2 = 2$ and *kH*=2 show alternative zones of stability and instability with increasing values of $\lambda_{cr.}$. In the case of values of $\widehat{D}_2 > 3$ the bifurcation map simplifies showing a small unstable region which tends to diminish for progressively larger values of the electric field together with a upper branch that increases with the electric field. For $\widehat{D}_2 = 5$, the unstable region is confined to a maximum value of $\lambda_{ct.} = 0.62$ and *kH* less than the unity. At the same time the upper curves show a relatively small slope and move to higher values of critical stretches with increasing the electric field.

In a similar way, Figure 4 shows plots of $\lambda_{ct.}$ vs. *kH* with $m\Omega_1^* = -0.01$ and $h^* = 0.2$ for different values of the applied electric field. In the present case, the bifurcation map is fairly more complex. Figure 4a corresponds to the case where the electric field is absent. In this case, the merging value for the critical stretch is 0.6715. It is to be noted that for values of $\lambda_{cr.} \leq 0.428$ and $\lambda_{cr.} \geq 3.16$ the plots are meaningless due to the fact that, taking $m\Omega_1^* = -0.01$, for these values of the stretch, imaginary values of s in Eq. (17) are obtained. For a similar reason, the curves corresponding to the situation when the electric field is present, do not show indication below about $\lambda_{cr.} = 0.5$. In general, for moderate electric fields the unstable zones tend to decrease for vales of *kH* between 4 and 5 and for higher values of *kH* these zones tend to be open giving rise to a new unstable zone. For $\widehat{D}_2 = 1$ the first unstable zone closes at about *kH*=5.5 and the second unstable zone becomes more complex. For values of $\widehat{D}_2$ between 1.5 and 1.9 new stable zones appear above and below $\lambda_{cr.} = 1$ which for $\widehat{D}_2 > 2$ induce a broad zone of stability which increases to about $\widehat{D}_2 = 2.25$. For higher values of the electric field the stable region tends to diminish.

If one makes $m = 0$ in Eq. (6) the density of the free energy is given by

$$\omega^*(\lambda, D_3) = \Omega_1^*\left[(2\lambda^2 + \lambda^{-4} - 3) + h^*(2\lambda^{-2} + \lambda^4 - 3) + \frac{\beta}{2\varepsilon_0\Omega_1^*}D_3^2\right] \qquad (21)$$

where, as above, $h^* = \frac{\Omega_2^*}{\Omega_1^*}$ (recalling that $D_3 = \lambda^{-2}D_{L3}$).

then Eq. (12) reduces to

$$\sum_{j=1}^{6}\left[(\lambda^{-4}(1 + h^*\lambda^2) + \widehat{D}_2^2)(1 + s_j^2)A_j - \widehat{D}_2 s_j\hat{B}_j\right] = 0$$

$$\sum_{j=1}^{6}\left\{\left[(\lambda^2 + 2\lambda^{-4})(1 + h^*\lambda^2) + \widehat{D}_2^2 - \left[\lambda^{-4}(1 + h^*\lambda^2) + \widehat{D}_2^2\right]s_j^2\right]s_jA_j - \widehat{D}_2(2 - s_j^2)\hat{B}_j\right]\right\} = 0$$

$$\sum_{1}^{6}\left[\widehat{D}_2(1 + s_j^2)A_j - s_j\hat{B}_j\right] = 0$$

$$\sum_{1}^{6}\left[(\lambda^{-4}(1 + h^*\lambda^2) + \widehat{D}_2^2)(1 + s_j^2)A_j - \beta\widehat{D}_2 s_j\hat{B}_j\right] e^{-ks_jh} = 0$$

$$\sum_{j=1}^{6}\left\{\left[(\lambda^2 + 2\lambda^{-4})(1 + h^*\lambda^2) + \widehat{D}_2^2 - \left[\lambda^{-4}(1 + h^*\lambda^2) + \widehat{D}_2^2\right]s_j^2\right]s_jA_j - \widehat{D}_2(2 - s_j^2)\hat{B}_j\right]\right\}e^{-ks_jh} = 0$$

$$\sum_{1}^{6}\left[\widehat{D}_2(1 + s_j^2)A_j - s_j\hat{B}_j\right]e^{-ks_jh} = 0$$

(22)

and the roots of Eq. (13) give

$$s_1 = 1\ (double),\ s_2 = -1\ (double),\ s_3 = \lambda^3,\ s_3 = -\lambda^3 \qquad (23)$$

Then, according to the strategy outlined in [14], the corresponding bifurcation equation is obtained and subsequently the bifurcation maps.

In Figure 5, plots of $\lambda_{crit.}$ vs. kH are shown. As expected, these plots are close to those of Figure 3 of Ref. [14].

It should be noted that when the electric field is absent, $\left(\widehat{D}_2 = 0\right)$, the factor $(1 + h^*\lambda^2)$ cancel in the main equations, the matrix obtained to find the unstable zones is reduced to a 4x4 one and the corresponding stability plot is exactly the obtained in Figure 3a of [14]. In this case, the equation giving the bifurcation map obtained from the cancellation of the corresponding determinant can be easily evaluated in a closed form to give

$$[16\lambda^6 + (\lambda^6 + 1)^4] \sinh(kH) \sinh(kH\lambda^3) - 8\lambda^3(\lambda^6 + 1)^2(\cosh(kH)\cosh(kH\lambda^3) - 1) \tag{24}$$

It is noticeable that since the term $(1 + h^*\lambda^2)$ is specifically due to the two parameter Mooney-Rivlin model, the cancellation of this factor reduces the stability behaviour and the bifurcation map to that obtained by using the neo-Hookean model. This conclusion is the opposite when the study of the stability and bifurcation phenomena of a square plate is set in terms of two equal biaxial forces in the 1 and 3 directions also in the absence of electric field [17]. This fact reveals not only the significant differences in the predictions of the two methods of analysis considered in this paper, but also the different results obtained when the sample is attacked by tension instead of deformation.

3.2. Comparison with the Hessian approach.

It is interesting to compare the preceding results with those obtained via the hessian approach. For equibiaxial deformation the Hessian matrix is given by

$$\begin{bmatrix} \frac{\partial^2\omega^*}{\partial\lambda^2} & \frac{\partial^2\omega^*}{\partial\lambda\partial D_{L2}} \\ \frac{\partial^2\omega^*}{\partial D_{L2}\partial\lambda} & \frac{\partial^2\omega^*}{\partial D_{L2}^2} \end{bmatrix} \tag{25}$$

The system is stable if the determinant of the Hessian matrix is positive.

From the Eq. (6) the determinant of the matrix (25) leads to

$$8{\Omega_1^*}^2\beta\lambda^{-4}[(\lambda^6 + 5) + 3h^*(\lambda^8 + \lambda^2) + m\Omega_1^*\Big((6\lambda^8 - 3\lambda^6 + 3\lambda^2 + 9\lambda^{-4} - 15) + h^*(15\lambda^{10} - 9\lambda^8 - 3\lambda^6 - 9\lambda^2 + 21\lambda^{-2} - 15) + 3{h^*}^2(7\lambda^{12} - 9\lambda^8 + \lambda^6 - 9\lambda^2 + 10)\Big) - 3\beta\lambda^4\widehat{D}_2^2] \tag{26}$$

Equalizing the expression (26) to zero and taking $\beta = 0.5$ and $h^* = 0.2$ the critical values for the stretch can be obtained from a plot $m\Omega_1^*$ vs λ for several values of $\widehat{D}_2$ (Figure 6) as follows

$$m\Omega_1^* = \frac{1.5\lambda^4\widehat{D}_2^2 - [(\lambda^6+5)+0.6(\lambda^8+\lambda^2)]}{\left[\begin{array}{c}(6\lambda^8-3\lambda^6+3\lambda^2+9\lambda^{-4}-15)+0.2(15\lambda^{10}-9\lambda^8-3\lambda^6-9\lambda^2+21\lambda^{-2}-15)+\\ +0.12(7\lambda^{12}-9\lambda^8+\lambda^6-9\lambda^2+10)\end{array}\right]} \quad (27)$$

From Eq. (27) it is possible to estimate for values of $m\Omega_1^*$and $\widehat{D_2}$ the stability limits in terms of the stretching λ . A comparison of the Figures (2) and (6) shows the differences between the two method used in the bifurcation analysis.

4. Ogden model.

The free energy of the model proposed by Ogden can be adequately represented by the following equation

$$\omega^*(\lambda_1,\lambda_2,\lambda_3) = \sum_{p=1}^{N}\frac{\mu_p}{\alpha_p}(\lambda_1^{\alpha_p}+\lambda_2^{\alpha_p}+\lambda_3^{\alpha_p}-3) \quad (28)$$

For equibiaxial deformations, taking N=3, and adding the electrostatic energy term one obtains:

$$\omega^*(\lambda, D_{L2}) = \sum_{p=1}^{3}\frac{\mu_p}{\alpha_p}(2\lambda^{\alpha_p}+\lambda^{-2\alpha_p}-3)+\frac{\beta}{2\varepsilon_0}\lambda^{-4}D_{L2}^2 \quad (29)$$

In order to be more specific the following values for α_p are adopted

$$\alpha_1 = 2, \alpha_2 = 4, \alpha_3 = -2 \quad (30)$$

from which the free energy reduces to

$$\omega^*(\lambda, D_{L2}) = \frac{\mu_1}{2}\left[(I_1-3)+\frac{h_1^*}{2}(I_1^2-2I_2-3)-h_2^*(I_2-3)+\frac{\beta}{\varepsilon_0\mu_1}\lambda^{-4}D_{L2}^2\right] \quad (31)$$

where $h_1^* = \frac{\mu_2}{\mu_1}, h_2^* = \frac{\mu_3}{\mu_1}$ and the definitions for the first and second invariants are taken into account.

By using Eq. (B14) the following expressions for the material parameters are obtained

$$a = 2\Omega_1^*\lambda^2 + 2\Omega_2^*\lambda^4; 2b = 2(\lambda^2+\lambda^{-4})(\Omega_1^*+\lambda^2\Omega_2^*)+4\Omega_{11}^*(\lambda^2-\lambda^{-4})^2+\frac{2\beta}{\varepsilon_0\mu_1}\lambda^{-4}D_{L2}^2; c = 2\Omega_1^*\lambda^{-4}+2\Omega_2^*\lambda^{-2}+\frac{2\beta}{\varepsilon_0\mu_1}\lambda^{-4}D_{L2}^2; d = \frac{2\beta}{\varepsilon_0}\lambda^{-2}D_{L2}; e = 2d; f = g = \frac{2\beta}{\varepsilon_0} \quad (32)$$

where $\Omega_1^* = \frac{\mu_1}{2}(1+h_1^*I_1); \Omega_2^* = -\frac{\mu_1}{2}(h_1^*+h_2^*); \Omega_{11}^* = \frac{\mu_1}{2}h_1^*; \Omega_5^* = \frac{\beta}{\varepsilon_0}$

the remaining terms being nil.

Dividing by $\frac{\mu_1}{2}$ and taking for simplicity $h_1^* = -h_2^* = h^*$, Eq. (B16) can be solved to give the following roots

$$s_1 = -s_2 = 1$$

$$s_3 = -s_4 = \frac{1}{2^{1/2}} \left\{ \begin{array}{c} \left(\lambda^6 + 1 + \dfrac{h^*(\lambda^4 - \lambda^{-2})^2}{1 + h^* I_1} \right) - \\ - \\ \left[\left(\lambda^6 + 1 + \dfrac{h^*(\lambda^4 - \lambda^{-2})^2}{1 + h^* I_1} \right)^2 - 4\lambda^6 \right]^{\frac{1}{2}} \end{array} \right\}^{\frac{1}{2}}$$

$$s_5 = -s_6 = \frac{1}{2^{1/2}} \left\{ \begin{array}{c} \left(\lambda^6 + 1 + \frac{h^*(\lambda^4 - \lambda^{-2})^2}{1 + h^* I_1} \right) + \\ + \\ \left[\left(\lambda^6 + 1 + \frac{h^*(\lambda^4 - \lambda^{-2})^2}{1 + h^* I_1} \right)^2 - 4\lambda^6 \right]^{\frac{1}{2}} \end{array} \right\}^{\frac{1}{2}} \qquad (33)$$

As above, in the absence of electric field the roots given by the Eq. (33) reduce to

$$s_1 = -s_2 = \frac{1}{2^{1/2}} \left\{ \begin{array}{c} \left(\lambda^6 + 1 + \dfrac{h^*(\lambda^4 - \lambda^{-2})^2}{1 + h^* I_1} \right) - \\ - \\ \left[\left(\lambda^6 + 1 + \dfrac{h^*(\lambda^4 - \lambda^{-2})^2}{1 + h^* I_1} \right)^2 - 4\lambda^6 \right]^{\frac{1}{2}} \end{array} \right\}^{\frac{1}{2}}$$

$$s_3 = -s_4 = \frac{1}{2^{1/2}} \left\{ \begin{array}{c} \left(\lambda^6 + 1 + \frac{h^*(\lambda^4 - \lambda^{-2})^2}{1 + h^* I_1} \right) + \\ + \\ \left[\left(\lambda^6 + 1 + \frac{h^*(\lambda^4 - \lambda^{-2})^2}{1 + h^* I_1} \right)^2 - 4\lambda^6 \right]^{\frac{1}{2}} \end{array} \right\}^{\frac{1}{2}} \qquad (34)$$

4.1. Results and Discussion.

In Figure 7, plots of λ_{cr} vs. kH for $h^* = 0.2$ and different values of the electric field are shown. The Figure 7a illustrates the case when the applied field is absent. A peak appears in the upper branch of the λ_{cr} vs. *kH* plots at about *kH=1* for $\widehat{D_2^2} > 1$. For values of the field higher than $\widehat{D_2^2} = 2.3$ two unstable regions appear in the bifurcation map, one for $\lambda_{cr} > 1$ and the other for $\lambda_{cr} < 1$. The first one broadens and tends to move to higher values of λ_{cr} with the electric field. On the contrary the second diminishes with the electric field as in the previous case. Clearly, the qualitative results of the analysis only are valid for the parameters given by Eq. (30). Further analysis for other parameters is now in progress.

4.2. Comparison with the Hessian approach.

In the present case the determinant of the matrix given by Eq. (25) leads to

$$\sum_{p=1}^{3}\mu_p\left[\left(\alpha_p-1\right)\lambda^{\alpha_p-2}+\left(2\alpha_p+1\right)\lambda^{-2\alpha_p-2}\right]-\frac{3\beta}{\varepsilon_0}\lambda^{-6}D_{L2}^2 \tag{35}$$

Eq. (35) with the chosen values for $\mu_{p}{}_{,}\alpha_p$ and taking, as above, $h_1^*=-h_2^*=h^*$ together with some simplification leads to

$$\lambda^4(\lambda^6+5)+3h^*(2\lambda^{12}+\lambda^6+1)=3\beta\lambda^8\widehat{D_2^2} \tag{36}$$

As above, equalizing Eq. (36) to zero and taking $h^*=0.2$ and $\beta=0.5$ a plot of the critical stretch versus $\widehat{D_2}$ are obtained as Figure 8 which is close to the Figure 4b of [14]. The differences between the two methods of analysis can also be understood at the sight of the Figure (8). This figure shows that for $\widehat{D_2}<2.12$ no instability occurs. For $\widehat{D_2}>2.12$ the electric field has a destabilizing effect, and a lateral stretch needs to be applied in order to prevent instability.

Summing up, the Hessian approach is purely constitutive and does not account for the plate thickness, thus resulting in a very different stability criterion from that based in the incremental formulation.

5. Conclusions.

Two main conclusions can be obtained from the preceding analysis. First, it is noticeable the striking contrast between the results obtained by means of the two methodologies to analyze the stability, the so-called hessian by one side and the incremental by the other, a fact stressed in [14]. The second is the inherent limitations of the empirical models used to represent the actual behaviour of these materials. It is obvious that more complex models must be chosen to better represent the actual behaviour. However, this fact, introduce new parameters, mostly unknown at present and makes the formal treatment more complicated. Under these conditions.it is advisable that many new questions can arise concerning the instability and bifurcation phenomena in electroelastic materials which opens a suggestive field for future research.

Acknowledgements.

R.D.C. thanks to Professor Ogden the suggestions made in preparing this manuscript.

Funding.

This research did not receive any specific grant from funding agencies in the public, commercial, or not-for-profit sectors.

6. References.

1) X. Zhao,W. Hong,Z. Suo,. *Electromechanical hysteresis and coexistent states in dielectric elastomers*. Phys. Rev B 76,134113, (2007).
2) X. Zhao,Z. Suo, *Method to analyze electromechanical stability of dielectric elastomers,* Appl. Phys. Lett. 91,061921, (2007).
3) M. Moscardo,X. Zhao,Z. Suo,Y. Lapusta, *Analysis and manufacture of an energy harvester based on a Mooney-Rivlin–type dielectric elastomer*. J.Appl. Phys.104,093503, (2008).
4) R. Diaz-Calleja,M.J. Sanchis,E. Riande, *Effect of an electric field on the deformation of incompressible rubbers: Bifurcation phenomena*. J. of Electrostatics, 67,158-166, (2009).
5) R. Diaz-Calleja,M.J. Sanchis,E. Riande, *Effect of an electric field on the bifurcation of a biaxially stretched incompressible slab rubber*. Eur. Phys. J. E, 30,417-426, (2009).
6) J. Leng,L. Liu,Y. Liu,S. Sun, Appl. Phys. *Electromechanical stability of dielectric elastomer*. Lett.94,211901, (2009).
7) Y. Liu,L. Liu,S. Sung,J. Leng, *Electromechanical stability of a Mooney–Rivlin-type dielectric elastomer with nonlinear variable permittivity*. Pol. International, 59,371-377, (2010).
8) Z. Suo, *Theory of dielectric elastomers*. Acta Mechanica Solida Sinica, 23,549-578, (2010).
9) J. Zhu,H. Stoyanov,G. Kofod,Z. Suo, *Large deformation and electromechanical instability of a dielectric elastomer tube actuator*. J. Appl. Phys., 108,074113, (2010).
10) B.X. Xu,R. Mueller,M. Klassen,D. Gross, *On electromechanical stability analysis of dielectric elastomer actuators*. Appl. Phys. Lett. 97,162908,(2010).
11) X. Zhao,S.J.A. Koh,Z. Suo, *Nonequilibrium thermodynamics of dielectric elastomers*. Int. J. Appl. Mech.,3,203-217,(2011).
12) S.M.A. Jimenez,R.M. McMeeking, *Deformation dependent dielectric permittivity and its effect on actuator performance and stability*. Int. J. of Non-Linear Mechanics 57,183-191,(2013).
13) A. Dorfmann, R.W. Ogden, *Nonlinear electroelastostatics: Incremental equations and stability*. Int. J. of Engn. Sci. 48,1-14,(2010).
14) Luis Dorfmann, R.W. Ogden, *Instabilities of an electroelastic plate*. Int. J. of Engn. Sci. 77,79-101,(2014).

15) A. Dorfmann,R.W. Ogden, *Nonlinear electroelasticity*. Acta Mechanica 174,167-183, (2005).
16) A.E. Green,W. Zerna, *Theoretical Elasticity*, Oxford U.P. (1954).
17) I-Shih Liu *Continuum Mechanics*, p. 159, Springer-Verlag, Berlin, (2002).
18) R. W. Ogden, *Non-linear Elastic Deformations*, Dover, N. York, (1984).

Appendix A. The basic equations governing nonlinear electroelasticity.

Finite electroelasticity.

Let us consider a deformable electroelastic system that in the stress-free reference configuration is denoted by $\mathcal{B}_r$ with boundary $\partial\mathcal{B}_r$. After the application of the mechanical and electrical force fields the material will have the configuration $\mathcal{B}$ with boundary $\partial\mathcal{B}_r$. In the absence of mechanical body forces the equilibrium equation in Eulerian form leads to

$$div\boldsymbol{\tau} = \mathbf{0} \tag{A1}$$

where $\boldsymbol{\tau}$ is the total Cauchy stress tensor satisfying the following boundary condition on any part of $\partial\mathcal{B}$

$$\boldsymbol{\tau n} = \boldsymbol{t}_a \tag{A2}$$

where $\mathbf{t}_a$ is the applied mechanical stress. Note that no Maxwell traction is assumed because the complient electrodes.

In absence of free charges inside the material the electromagnetic equations reduce to

$$div\boldsymbol{D}=0, \quad curl\boldsymbol{E} = \mathbf{0} \tag{A3}$$

In presence of a free charge σ_f per unit area of surface the boundary conditions are

$$\boldsymbol{n} \times \boldsymbol{E} = \mathbf{0}, \boldsymbol{n} \cdot \boldsymbol{D} = -\sigma_f \tag{A4}$$

It is more convenient to work in terms of a Lagrangian formulation. Thus, if one denotes respectively by $\boldsymbol{X}$ and $\boldsymbol{x}$ the material points in the reference and in the deformed configurations which are related via the function $\boldsymbol{\chi}$, such that $\boldsymbol{x} = \boldsymbol{\chi}(\boldsymbol{X})$. The second-order tensor $\boldsymbol{F} = Grad\,\boldsymbol{\chi}$ is the deformation gradient referred to $\boldsymbol{X}$. The total nominal stress tensor $\boldsymbol{T}$ is defined by $\boldsymbol{T} = J\boldsymbol{F}^{-1}\boldsymbol{\tau}$, where $J = det\boldsymbol{F}$, satisfying the equilibrium equation.

$$Div\boldsymbol{T} = \mathbf{0} \tag{A5}$$

In the case of incompressible materials, one has $J = 1$.

The corresponding boundary condition is

$$\boldsymbol{T}^T\boldsymbol{N} = \boldsymbol{t_A} + \boldsymbol{T}_E^{\star T}\boldsymbol{N}, \quad \boldsymbol{T}_E^{\star} = J\boldsymbol{F}^{-1}\boldsymbol{\tau}_{\boldsymbol{e}}^{\star} \tag{A6}$$

on $\partial\mathcal{B}_r$, where ^{T} means the transpose of a second-order tensor and $\mathbf{N}$ is the unit outward normal to $\partial\mathcal{B}_r$.

The (nominal) electric field $\boldsymbol{E}_L$ and electric displacement $\boldsymbol{D}_L$ are defined now as

$$\boldsymbol{E}_L = \boldsymbol{F}^T\boldsymbol{E}, \quad \boldsymbol{D}_L = J\boldsymbol{F}^{-1}\boldsymbol{D} \tag{A7}$$

where the subscript L is referred to the Lagrangian formulation

These satisfy the following field equations

$$Div\,\boldsymbol{D}_L = 0, \quad Curl\,\boldsymbol{E}_L = \mathbf{0} \tag{A8}$$

where the capitals indicate that the vector operators are taken with respect to $\boldsymbol{X}$.

The corresponding boundary conditions in Lagrangian form are given by

$$\boldsymbol{N}\cdot\boldsymbol{D_L}=-\sigma_{\boldsymbol{F}},\ \ \boldsymbol{N}\times\boldsymbol{E}_L=\boldsymbol{0} \tag{A9}$$

where $\sigma_{\boldsymbol{F}}$ is the free charge density per unit area of $\partial\mathcal{B}_r$.

A total free energy density function $\Omega^*(\boldsymbol{F},\boldsymbol{D}_L)$ is assumed from which for such incompressible material ($\det\boldsymbol{F}=1$).

$$T=\frac{\partial\Omega^*}{\partial\boldsymbol{F}}-p^*\boldsymbol{F}^{-1},\boldsymbol{E}_L=\frac{\partial\Omega^*}{\partial\boldsymbol{D}_L},\boldsymbol{\tau}=\boldsymbol{F}\frac{\partial\Omega^*}{\partial\boldsymbol{F}}-p^*\boldsymbol{I},\boldsymbol{E}=\boldsymbol{F}^{-\boldsymbol{T}}\frac{\partial\Omega^*}{\partial\boldsymbol{D}_L} \tag{A10}$$

Where $p^*$is a Lagrange multiplier coming from the incompressibility condition.

Of course other definitions for the free energy function are possible as referred in Ref. [15].

For isotropic electroelastic materials $\Omega^*$is an isotropic function of the tensors $\boldsymbol{C}=\boldsymbol{F}^T\boldsymbol{F}$ and $\boldsymbol{D}_L\otimes\boldsymbol{D}_L$. In the case of incompressible materials the dependence of Ω^* is reduced to the following invariants

$$I_1=Tr\boldsymbol{C},\ \ I_2=\frac{\boldsymbol{1}}{\boldsymbol{2}}[(Tr\boldsymbol{C})^{\boldsymbol{2}}-(Tr\boldsymbol{C}^{\boldsymbol{2}})],\ \ I_4=|\boldsymbol{D}_L^2|,\ \ I_5=\boldsymbol{D}_L\cdot(\boldsymbol{C}\boldsymbol{D}_L),\ \ I_6=\boldsymbol{D}_L\cdot(\boldsymbol{C}^2\boldsymbol{D}_L) \tag{A11}$$

where Tr is the trace of a second order tensor.

Then, one can set $\Omega^*=\Omega^*(I_1,I_2,I_4,I_5,I_6)$, and from the Eq. (A10) the total stress and the electric field are obtained in the Eulerian forms

$$\boldsymbol{\tau}=\boldsymbol{2}\Omega_1^*\boldsymbol{B}+\boldsymbol{2}\Omega_2^*(I_1\boldsymbol{B}-\boldsymbol{B}^2)-p^*\boldsymbol{I}-\boldsymbol{2}\Omega_5^*\boldsymbol{D}\otimes\boldsymbol{D}+\boldsymbol{2}\Omega_6^*[\boldsymbol{D}\otimes\boldsymbol{BD}+\boldsymbol{BD}\otimes\boldsymbol{D}]$$
$$\boldsymbol{E}=2(\Omega_4^*\boldsymbol{B}^{-\boldsymbol{1}}\boldsymbol{D}+\Omega_5^*\boldsymbol{D}+\Omega_6^*\boldsymbol{BD}) \tag{A12}$$

where Ω_i^* is defined as $\frac{\partial\Omega^*}{\partial I_i}$ for $i=1{,}2{,}4{,}5{,}6$

The Lagrangian counterparts are obtained from $\boldsymbol{T}=\boldsymbol{F}^{-1}\boldsymbol{\tau},\ \ \boldsymbol{E_L}=\boldsymbol{F^T}\boldsymbol{E}$.

Appendix B. Incremental formulation.

Following the notation of Ref. [14], an increment in a variable will be represented by a superposed dot.

For the forthcoming analysis it is convenient to update the variables in such a way that $\mathcal{B}$ becomes the reference configuration. The resulting variables will be identified with a subscript 0 and, consequently, one has

$$\dot{\boldsymbol{E}}_{L0}=\boldsymbol{F}^{-T}\dot{\boldsymbol{E}}_L,\ \ \dot{\boldsymbol{D}}_{L0}=\boldsymbol{F}\dot{\boldsymbol{D}}_L,\ \ \dot{\boldsymbol{T}}_0=\boldsymbol{F}\dot{\boldsymbol{T}} \tag{B1}$$

The incremental equations are updated to

$$div\,\dot{\boldsymbol{D}}_{L0}=0,\ \ curl\,\dot{\boldsymbol{E}}_{L0}=\boldsymbol{0},\ div\,\dot{\boldsymbol{T}}_0=\boldsymbol{0} \tag{B2}$$

and, after the pertinent calculations, the following incremental forms of the traction and electrical boundary conditions for incompressible materials now on $\partial\mathcal{B}$ lead to

$$\dot{\boldsymbol{T}}_0^T\boldsymbol{n} = \dot{\boldsymbol{t}}_{A0} \quad on \;\; \partial\mathcal{B}$$
$$\dot{\boldsymbol{D}}_{L0}\cdot\boldsymbol{n} = -\dot{\sigma}_{F0} \quad on \;\; \partial\mathcal{B} \tag{B3}$$
$$\dot{\boldsymbol{E}}_{L0}\times\boldsymbol{n} = \boldsymbol{0} \quad on \;\; \partial\mathcal{B}$$

where $\dot{\sigma}_{F0} = \dot{\sigma}_F\frac{dA}{da}$ is the increment of free surface charge. The incremental incompressibility condition leads to

$$div\mathbf{u} = 0 \tag{B4}$$

Let us consider now an incremental deformation $\dot{\boldsymbol{F}}$ superimposed to an increment in the Lagrangian electric field $\dot{\boldsymbol{D}}_L$ in the configuration $\mathcal{B}$. Then, the linear incremental expressions for $\dot{\boldsymbol{T}}_0$ and $\dot{\boldsymbol{E}}_{L0}$ for an unconstrained and incompressible material in the Eulerian form, are [14]

$$\dot{\boldsymbol{T}}_0 = \boldsymbol{\mathcal{A}}_0^*\boldsymbol{L} + \mathbb{A}\dot{\boldsymbol{D}}_{L0} + p^*\boldsymbol{L} - \dot{p}^*\boldsymbol{I}, \;\; \dot{\boldsymbol{E}}_{L0} = \mathbb{A}_{\boldsymbol{0}}^{*T}\boldsymbol{L} + \boldsymbol{A}_{\boldsymbol{0}}^*\dot{\boldsymbol{D}}_{L0} \tag{B5}$$

where $\boldsymbol{L} = grad\;\boldsymbol{u}$ and $\boldsymbol{\mathcal{A}}_0^*, \mathbb{A}_0^*, \boldsymbol{A}_0^*$ are, respectively, the fourth-,third- and second-order electroelastic moduli tensors associated with the total energy $\Omega^*(\boldsymbol{F},\boldsymbol{D}_L)$.

These can be writen in component form for incompressible materials as

$$\mathcal{A}_{0jikl}^* = F_{j\alpha}F_{l\beta}\frac{\partial^2\Omega^*}{\partial F_{i\alpha}\partial F_{j\beta}}, \;\; \mathbb{A}_{0\alpha i|\beta}^* = \frac{\partial^2\Omega^*}{\partial F_{i\alpha}\partial D_{L\beta}}, \;\; A_{\alpha\beta}^* = \frac{\partial^2\Omega^*}{\partial D_{L\alpha}\partial D_{L\beta}} \tag{B6}$$

The vertical bar between the indices in the second equation (B6), is used to distinguish the single subscript from the pair of subscripts going together. The following symmetry conditions for these tensors are fulfilled [15]

$$\mathcal{A}_{0\alpha i\beta j}^* = \mathcal{A}_{0\beta j\alpha i}^*, \;\; \mathbb{A}_{0ij|k}^* = \mathbb{A}_{0ji|k}^*, \;\; A_{0\alpha\beta}^* = A_{0\beta\alpha}^* \tag{B7}$$

It is to be noted that for an unconstrained electroelastic material Ω^* is a function of the six invariants $I_1,\dots,I_6$ and Eq. (B 6) can be expanded in terms of the first and second order derivatives of the invariants (e.g. Eq. (28) of Ref. [13]).

The next step is to specialize the incremental formulation derived in Appendix B for the specific geometry of our problem. For this purpose, taking into account that the deformation is equibiaxial the incremental displacement will be a plane strain in the (x_1, x_2) plane. The incremental displacement vector will be $\boldsymbol{u} = (u_1, u_2, 0)$ which only depend on x_1 and x_2. Thus, the incompressibility condition reduces to

$$u_{1,1} + u_{2,2} = 0 \tag{B8}$$

where as usual a comma in the subscript indicates partial differentiation with respect the corresponding variable.

In analogy, one defines $\dot{\boldsymbol{D}}_{L0} = (\dot{D}_{L01}, \dot{D}_{L02}, 0)$ with components that depend only on x_1 and x_2.These components must satisfy the first equation of (B2), that is

$$\dot{D}_{L01,1} + \dot{D}_{L02,2} = 0 \tag{B9}$$

Eq. (B8, B9) predict the existence of functions $\psi = \psi(x_1, x_2)$ and $\varphi = \varphi(x_1, x_2)$ in such a way that

$$u_1 = \psi_{,2},\ \ u_2 = -\psi_{,1} \text{ and } \dot{D}_{L01} = \varphi_{,2},\ \ \dot{D}_{L02} = -\varphi_{,1} \tag{B10}$$

and $\varphi_{,11} + \varphi_{,22} = 0$ according to the Laplace equation.

From the third and the second equations in (B2), one obtains

$$\dot{T}_{011,1} + \dot{T}_{021,2} = 0,\ \ \dot{T}_{012,1} + \dot{T}_{022,2}\ ,\dot{E}_{L01,2} - \dot{E}_{L02,1} = 0 \tag{B11}$$

where the components of $\dot{\boldsymbol{T}}_{\boldsymbol{0}}$ and $\dot{\boldsymbol{E}}_{L0}$ are obtained from Eq. (B5).

After the pertinent calculations, the updated incremental total nominal stress tensor and the Lagrangian electric displacement non-zero components can be easily calculated. The results as well as the incremental boundary conditions in terms of the functions ψ and φ are

$$(\mathcal{A}^*_{01111} - \mathcal{A}^*_{01221} - \mathcal{A}^*_{01122})\psi_{,112} + \mathcal{A}^*_{02121}\psi_{,222} - \mathbb{A}^*_{011|2}\varphi_{,11} + \mathbb{A}^*_{021|1}\varphi_{223} = \dot{p}^*_{,1}$$
$$(\mathcal{A}^*_{02222} - \mathcal{A}^*_{01122} - \mathcal{A}^*_{01221})\psi_{,122} + \mathcal{A}^*_{01212}\psi_{,111} - (\mathbb{A}^*_{012|1} - \mathbb{A}^*_{022|2})\varphi_{,12} = -\dot{p}^*_{,2}$$
$$\left(\mathbb{A}^*_{021|1+} + \mathbb{A}^*_{011|2} - \mathbb{A}^*_{022|2}\right)\psi_{,122} - \mathbb{A}^*_{021|1}\psi_{,111} + (A_{011} - A_{022})\varphi_{,12} = 0$$

(B12)

After elimination of $\dot{p}^*$ from the first two of these equations, one obtains a system of equations for ψ and φ which may be written in compact form as

$$a\psi_{,1111} + 2b\psi_{,1122} + c\psi_{,2222} + (e-d)\varphi_{,112} + d\varphi_{,222} = 0$$
$$(e-d)\psi_{,122} + d\psi_{,111} - (f-g)\varphi_{,12} = 0$$

(B13)

where

$$a = \mathcal{A}^*_{01212},\ \ 2b = \mathcal{A}^*_{01111} + \mathcal{A}^*_{02222} - 2\mathcal{A}^*_{01221} - 2\mathcal{A}^*_{01122}, \qquad c = \mathcal{A}^*_{02121}$$
$$d = \mathbb{A}^*_{021|1},\ \ e = \mathbb{A}^*_{022|2} - \mathbb{A}^*_{011|2},\ \ f = A_{011},\ \ g = A_{022}$$

(B14)

are material parameters.

Small-amplitude solutions have been chosen, among others, to solve the incremental boundary-value problem as in Ref. [14].

$$\psi = A\exp(-ksx_2)\exp(ikx_1),\ \ \varphi = kB\exp(-ksx_2)\exp(ikx_1) \tag{B15}$$

where s is to be determined and k is the wave-number of the signals.

Substitution of (B15) in (B13) and subsequent check for non-trivial solutions of the homogeneous system resulting leads to the following cubic equation in s^2

$$(cf-d^2)s^6-[2bf+cg+2(d-e)]s^4+[2bg+af-(d-e)^2]s^2-ag=0 \quad \text{(B16)}$$

The general solution for the plate may be written as $A_j\exp(-ks_jx_3)\exp(ikx_1)$

$$\psi=\sum_{j=1}^{6}A_j\exp(-ks_jx_2)\exp(ikx_1)\,,\;\; \varphi=k\sum_{j=1}^{6}B_j\exp(-ks_jx_2)\exp(ikx_1) \quad \text{(B17)}$$

The twelve unknown constants $A_j, B_j, j=1,\dots,6$ are not independent but they are related through the following equation

$$s_j(ds_j^2+d-e)A_j-(fs_j^2-g)B_j=0 \quad \text{(B18)}$$

For the configuration of compliant electrodes proposed in the Paragraph 2, remembering that there is no electric field outside the plate and assuming that neither applied nor incremental mechanical tractions are present, the incremental boundary conditions are

$$c(\psi_{,22}-\psi_{,11})+d\varphi_{,2}=0$$

$$on\; x_2=0,h$$

$$(2b+c)\psi_{,112}+c\psi_{,222}+e\varphi_{,11}+d\varphi_{,22}=0 \quad \text{(B19)}$$

The incremental electric boundary conditions reduce to

$$\dot{E}_{L01}=0,\;\; \dot{D}_{L02}=-\dot{\sigma}_{F0}\; on\; x_2=0,h \quad \text{(B20)}$$

which, after rewritten in terms of ψ,φ reduce to

$$d(\psi_{,22}-\psi_{,11})+f\varphi_{,2},\;\; \varphi_{,1}=\dot{\sigma}_{F0}\quad on\quad x_2=0,h \quad \text{(B21)}$$

Note that the field D_3 satisfy the jump condition $D_2=\sigma_f$ on $x_2=0,h$.

Substitution of (B17) in (B18), (B19) and (B21)$_1$ on the faces $x_2=0,h$, one obtains

$$\sum_{j=1}^{6}\left[c(1+s_j^2)A_j-ds_jB_j\right]=0$$

$$\sum_{j=1}^{6}\left[(2b+c-cs_j^2)s_jA_j-(e-ds_j^2)B_j\right]=0$$

$$\sum_{j=1}^{6}\left[d(1+s_j^2)A_j-fs_jB_j\right]=0$$

$$\sum_{j=1}^{6}\left[c(1+s_j^2)A_j-ds_jB_j\right]exp(-khs_j)=0$$

$$\sum_{j=1}^{6}\left[(2b+c-cs_j^2)s_jA_j-(e-ds_j^2)B_j\right]exp(-khs_j)=0$$

$$\sum_{j=1}^{6}\left[d\left(1+s_j^2\right)A_j - f s_j B_j\right]\exp(-khs_j) = 0 \tag{B22}$$

Eq. (B18) and (B22) form a homogeneous system of twelve linear equations for twelve unknowns. Non-trivial solutions are possible if the determinant of the coefficients of this system vanish. However, the size of the 12x12 determinant can be reduced to a 6x6 one by taking into account the relation between A_j and B_j.

Figure(s)

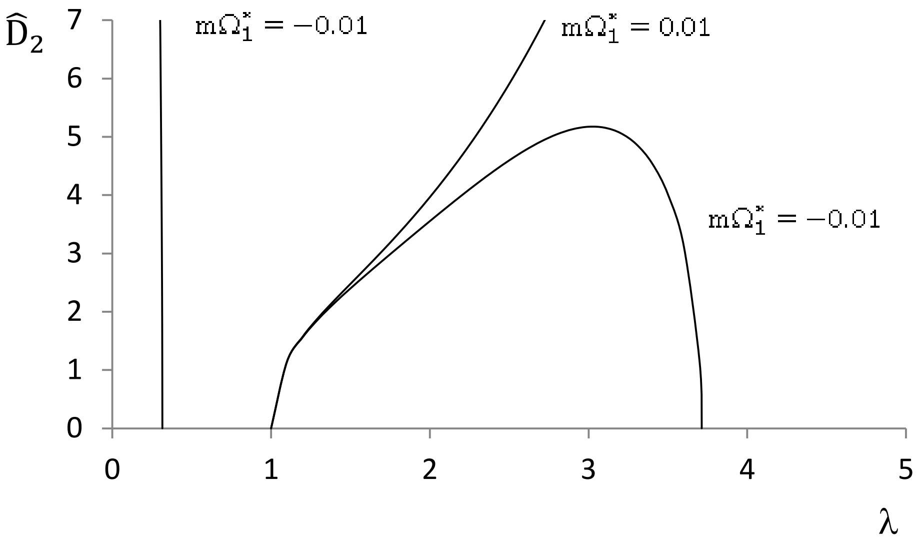

Figure 1. Plot of $\widehat{D}_2$ vs λ for β=0.5 and $m\Omega_1^* = \pm 0.01$.

Figure(s)

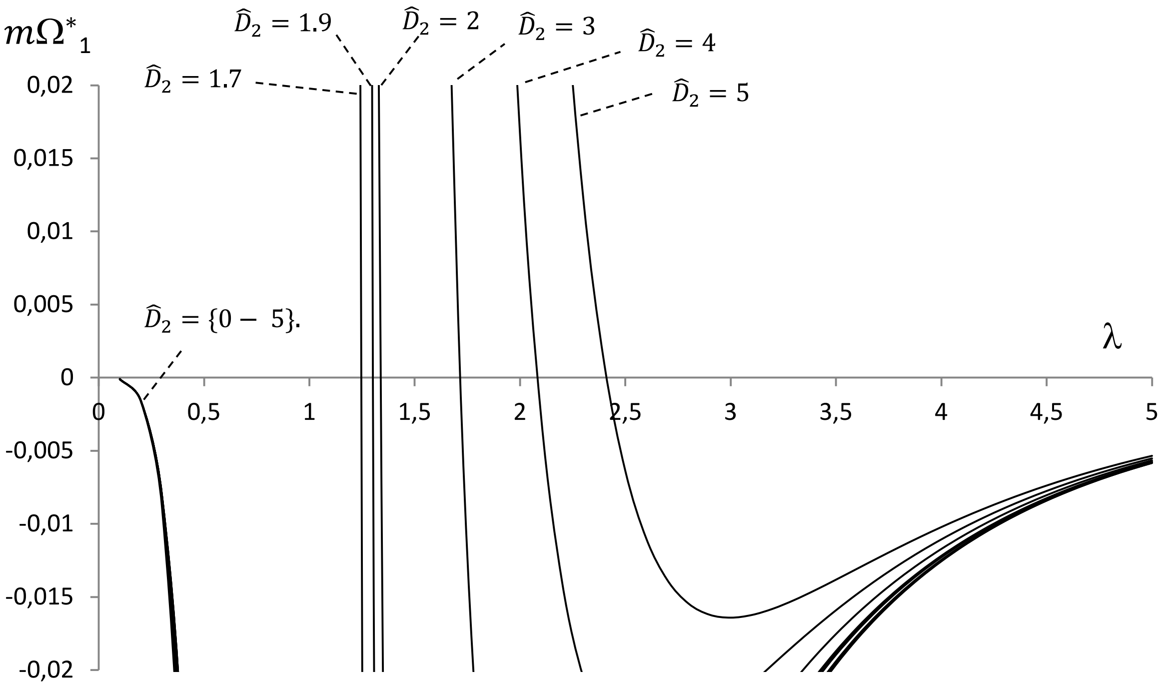

Figure 2. Plot of mΩ_1^* vs λ for β=0.5 and $\widehat{D}_2$=0, 0.1, 0.5, 1, 1.7, 1.9, 2, 3, 4, 5.

Figure(s)

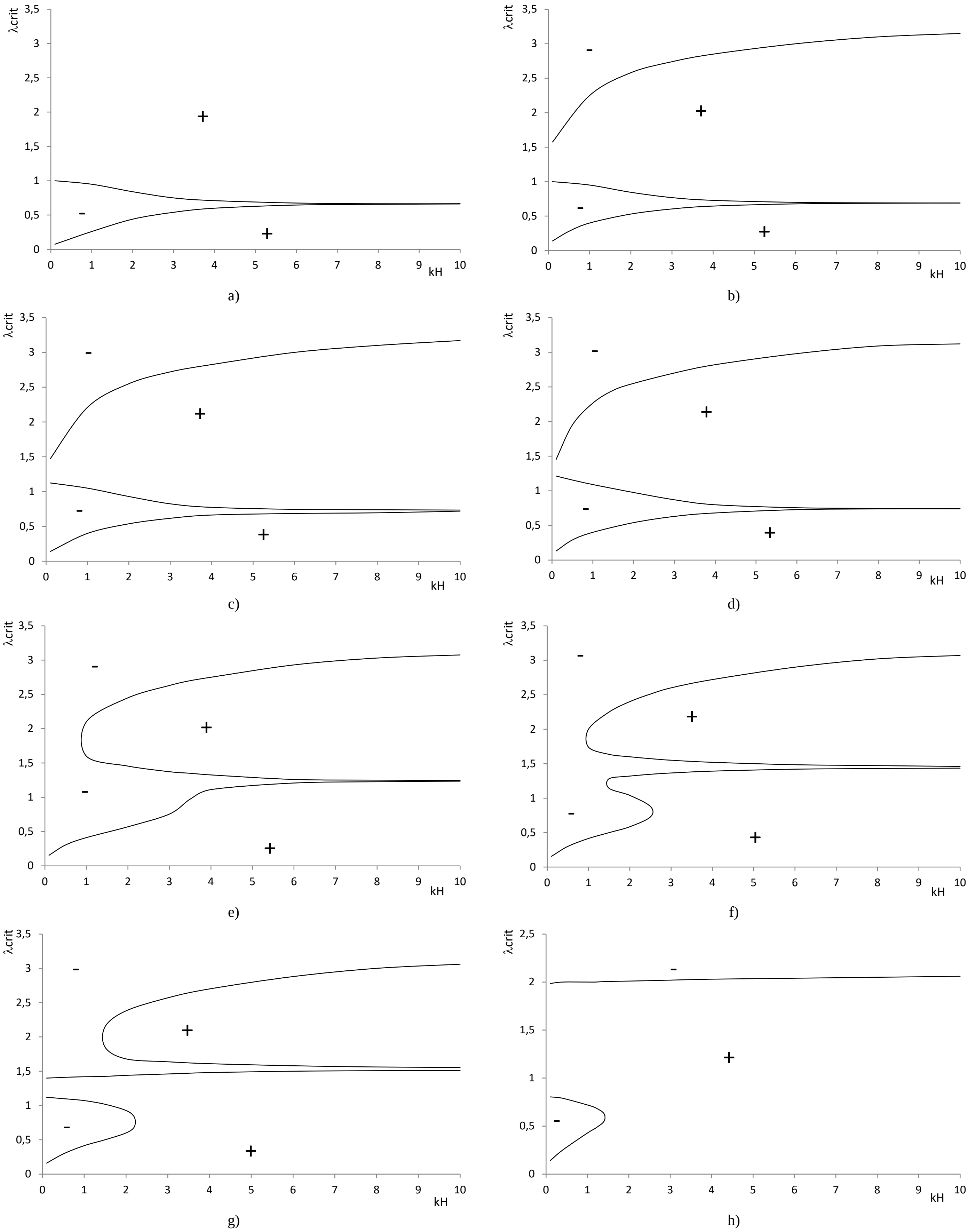

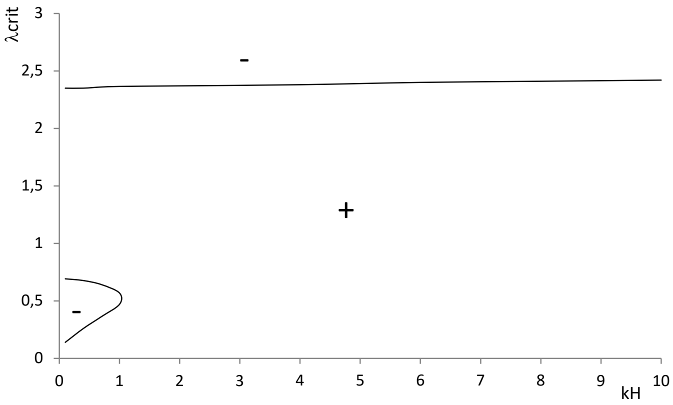

i)

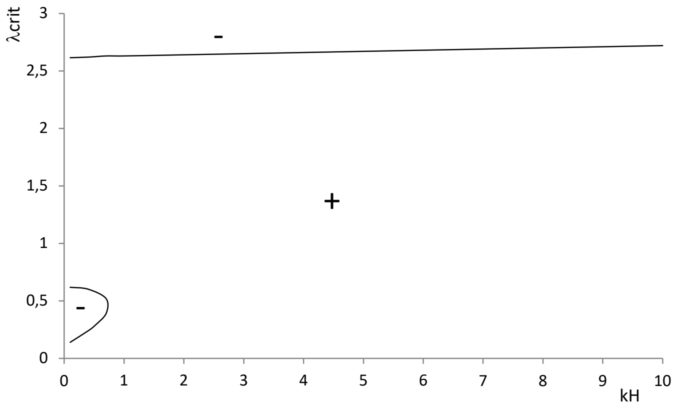

j)

Figure 3. Plots of λ_{cr} vs kH, m$\Omega_1^* = 0.01$ and $h^* = 0.2$ with values of $\widehat{D}_2$=0, 0.1, 0.5, 1, 1.7, 1.9, 2, 3, 4 and 5 in (a)-(j) respectively. (+) indicates stable behaviour and (-) unstable behaviour.

Figure(s)

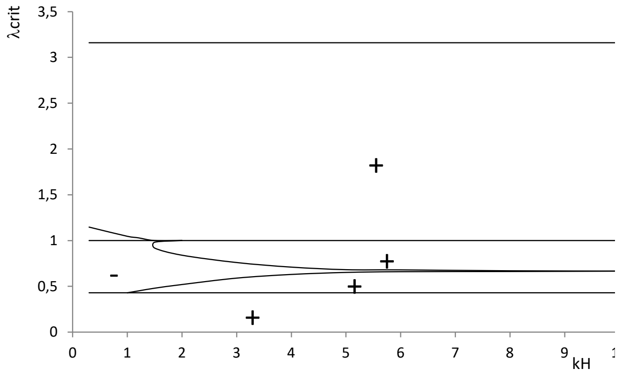

a)

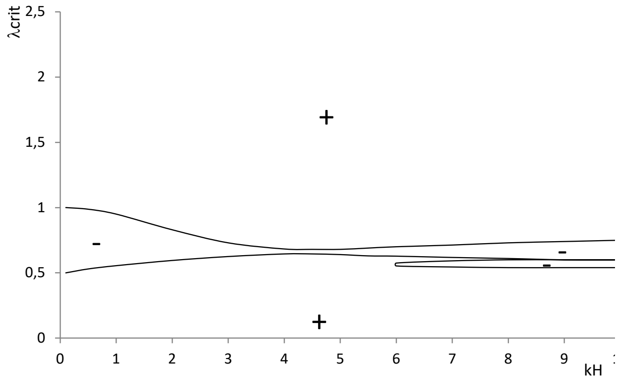

b)

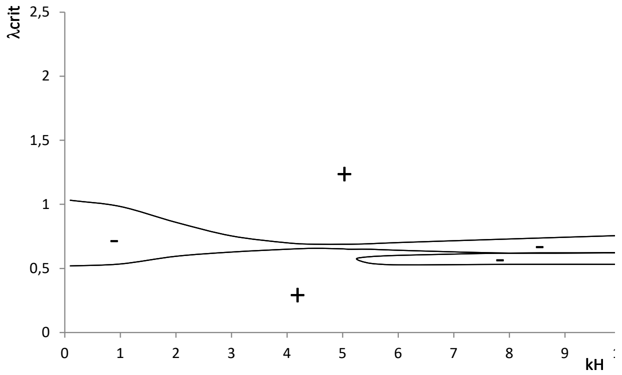

c)

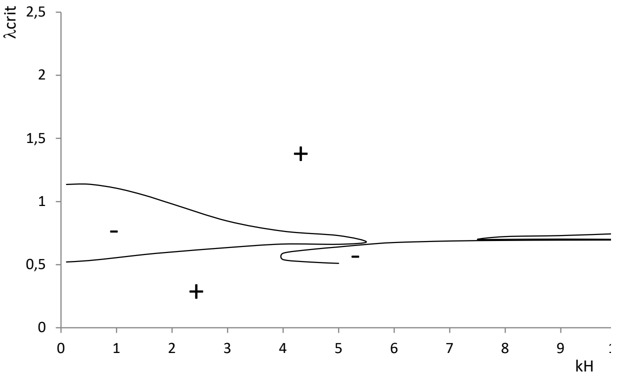

d)

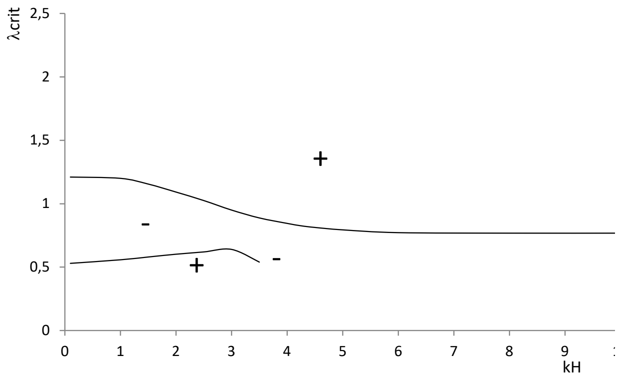

e)

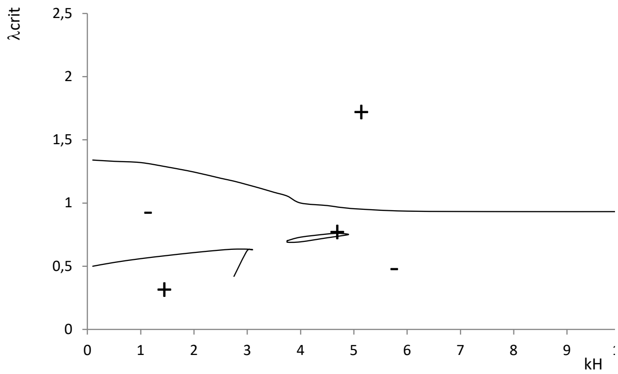

f)

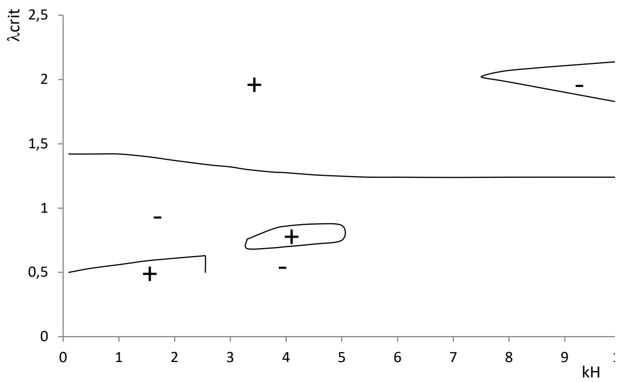

g)

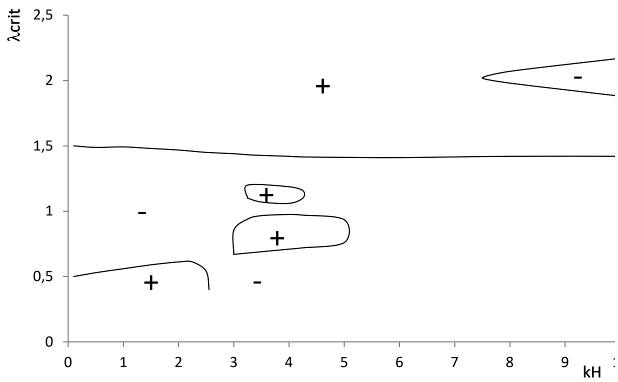

h)

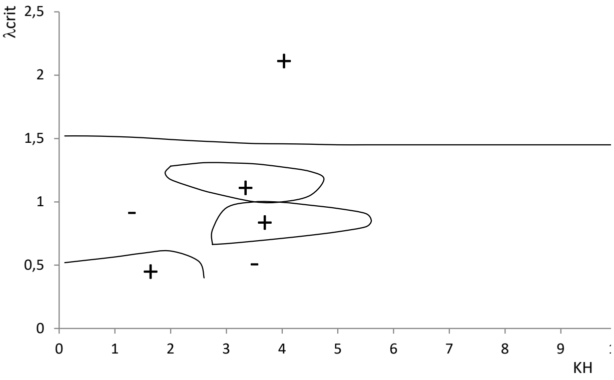
λcrit
kH

i)

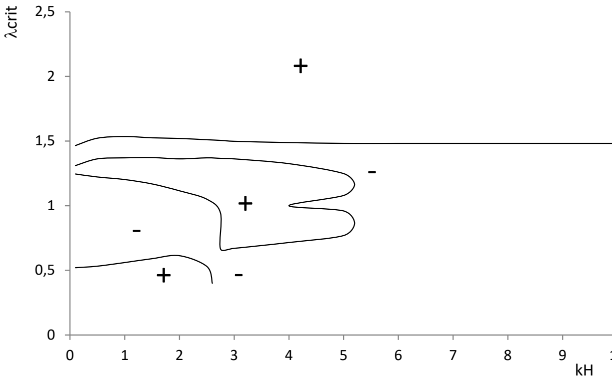
λcrit
kH

j)

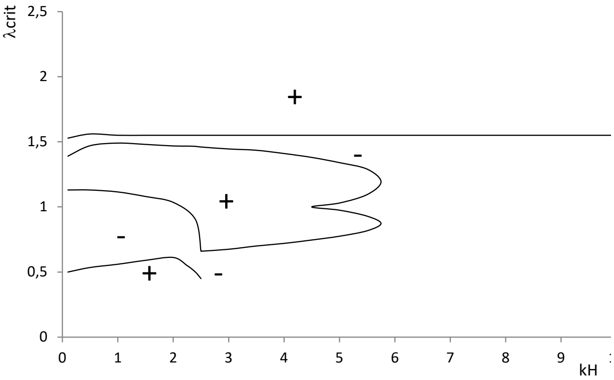
λcrit
kH

k)

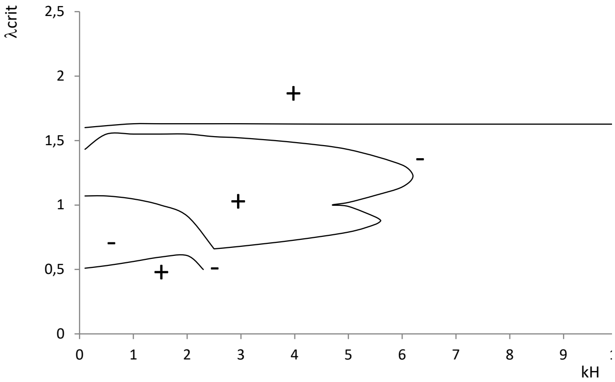
λcrit
kH

l)

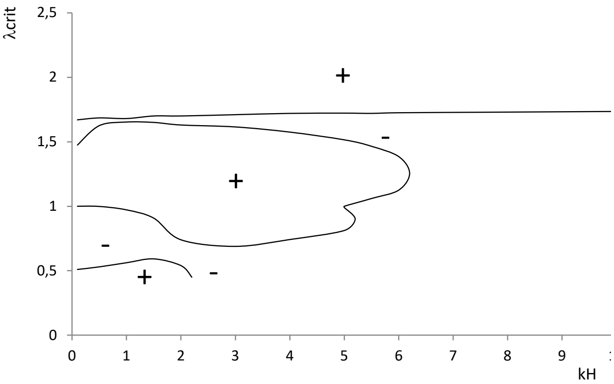
λcrit
kH

m)

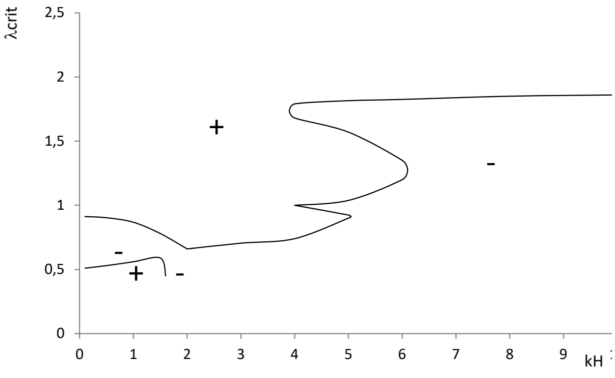
λcrit
kH

n)

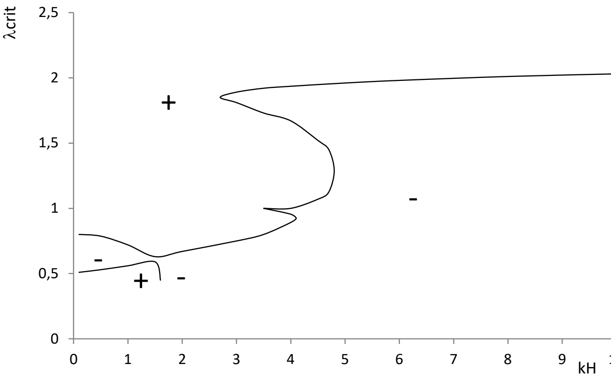
λcrit
kH

o)

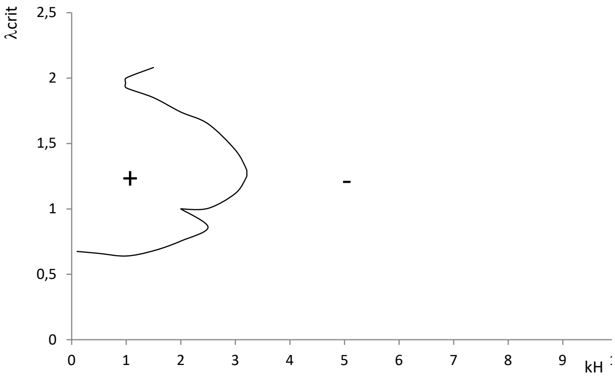
λcrit
kH

p)

q

Figure 4. Plots of λ_{cr} vs kH, m$\Omega_1^* = -0.01$ and $h^* = 0.2$ with values of $\widehat{D}_2$=0, 0.1, 0.5, 1, 1.25, 1.5, 1.7, 1.85, 1.89, 1.925 , 2, 2.1, 2.25, 2.5, 3, 4 and 5 in (a)-(r) respectively. (+) indicates stable behaviour and (-) unstable behaviour.

Figure(s)

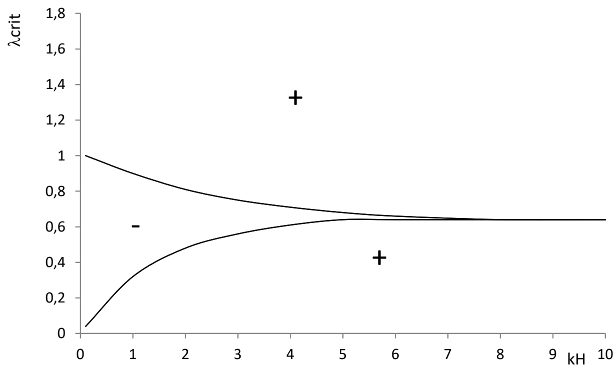

a)

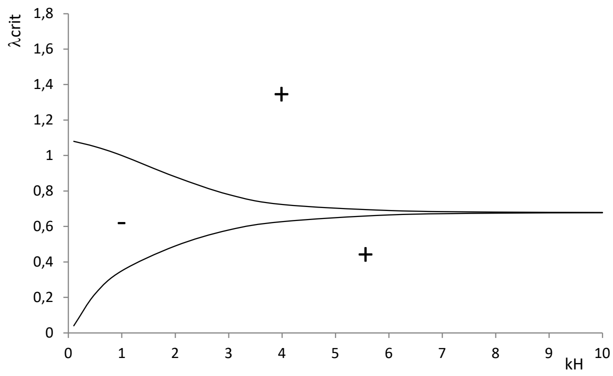

b)

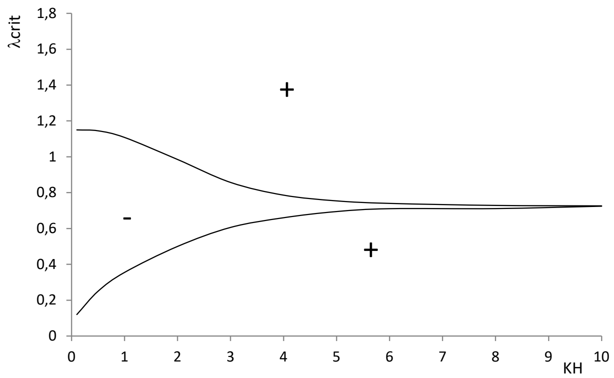

c)

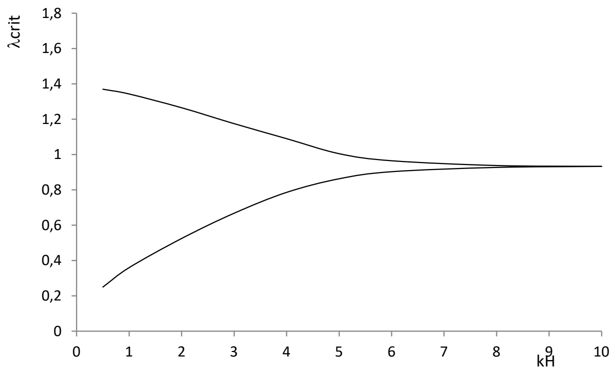

d)

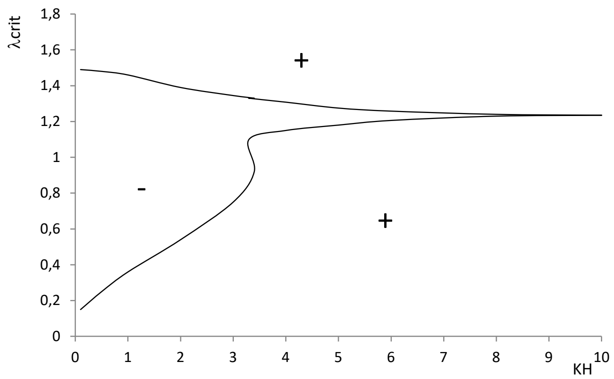

e)

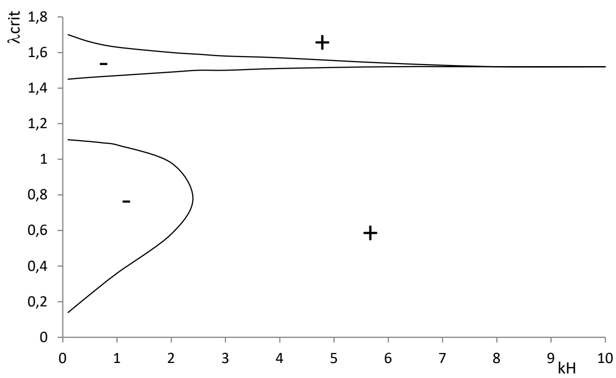

f)

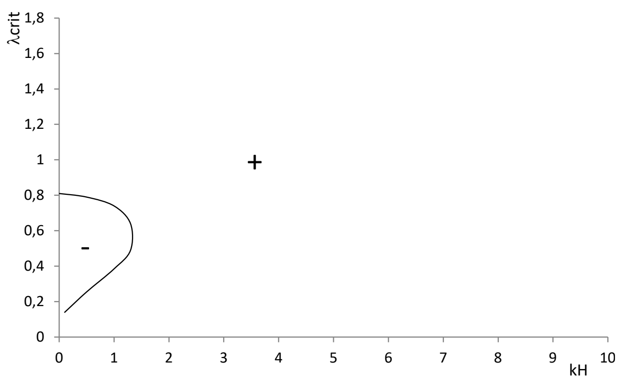

g)

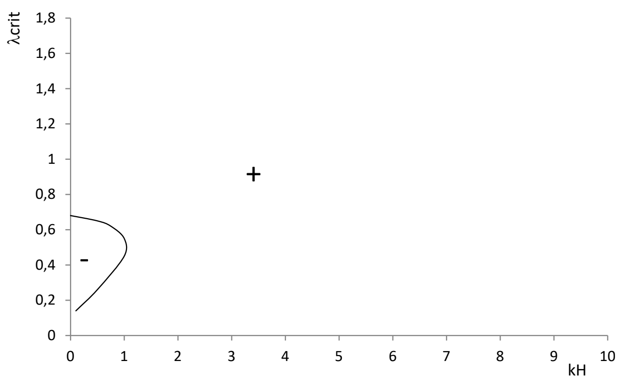

h)

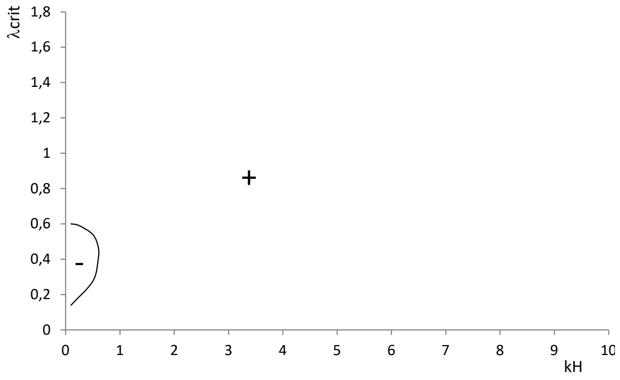

i)

Figure 5. Plots of λ_{cr} vs kH for the modified Mooney-Rivlin model, m$\Omega_1^* = 0$ and $h^* = 0.2$ with values of $\hat{D}_2$=0, 0.5, 1, 1.5, 1.7, 2, 3, 4 and 5 in (a)-(j) respectively. (+) indicates stable behaviour and (-) unstable behaviour.

Figure(s)

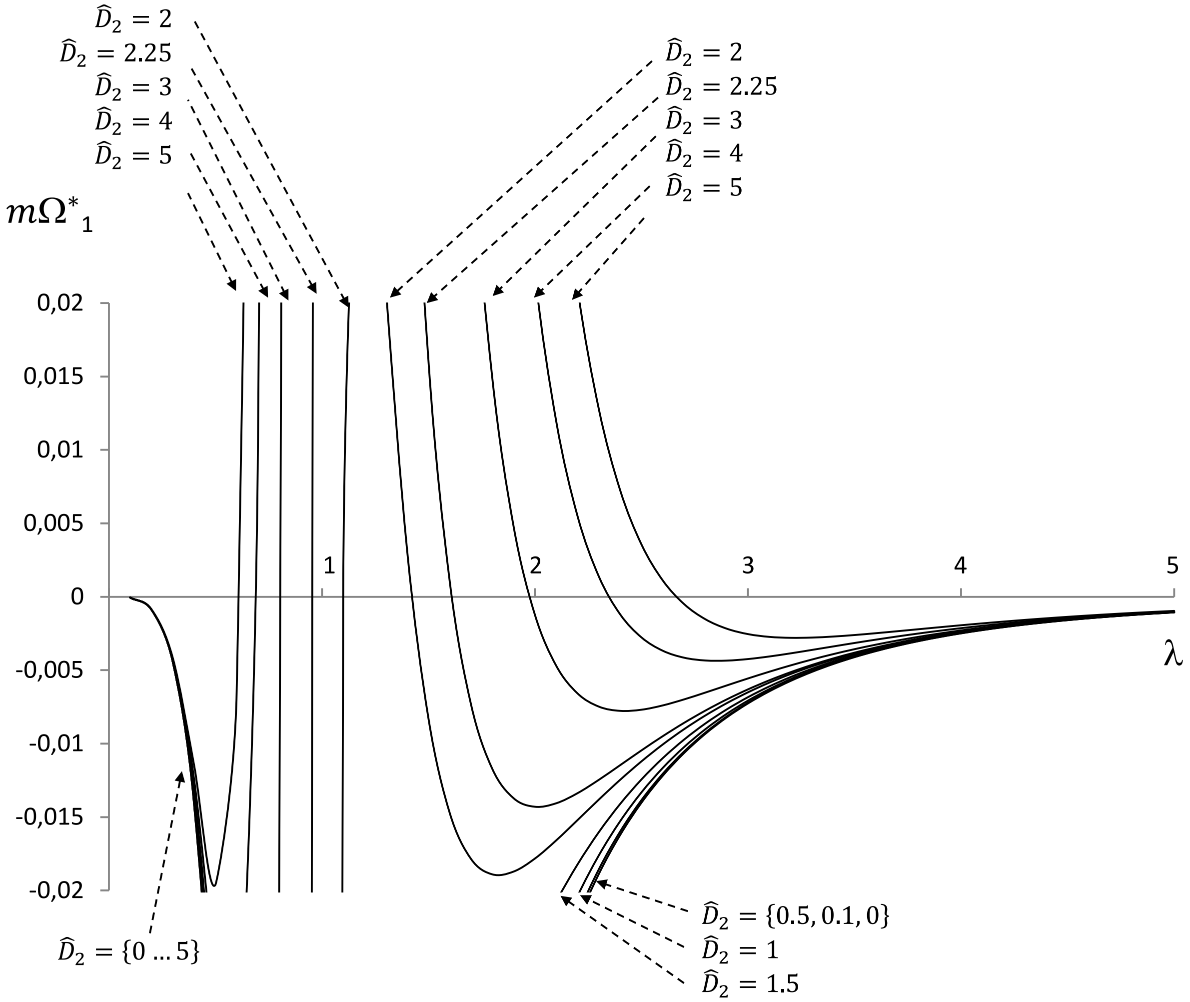

Figure 6. Plot of $m\Omega_1^*$ vs λ for several values of $\widehat{D}_2$.

Figure(s)

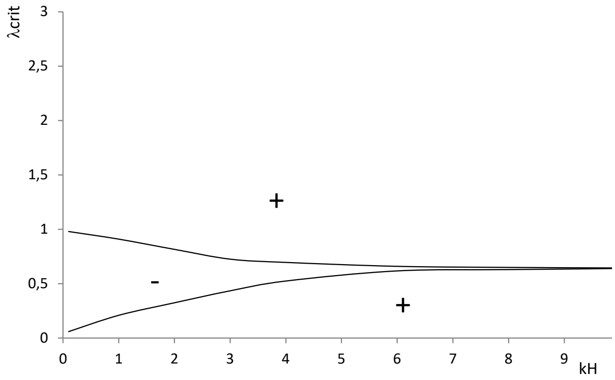

a)

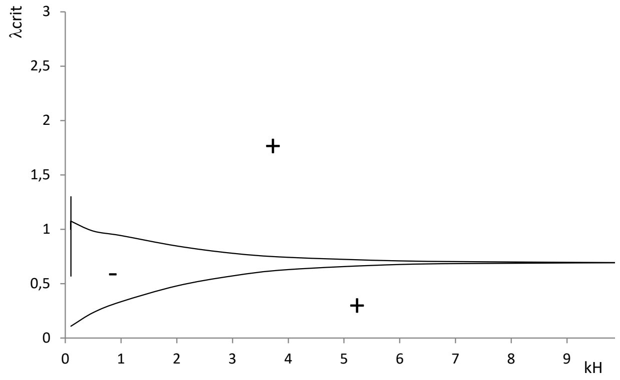

b)

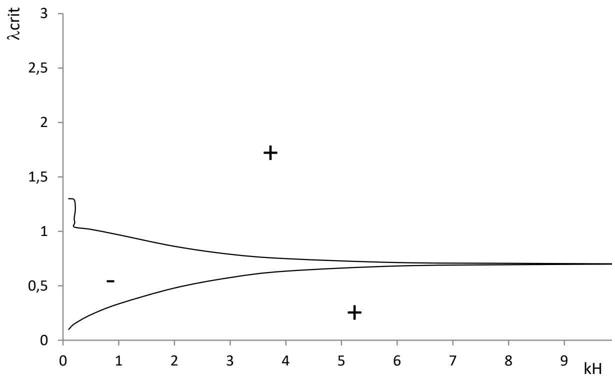

c)

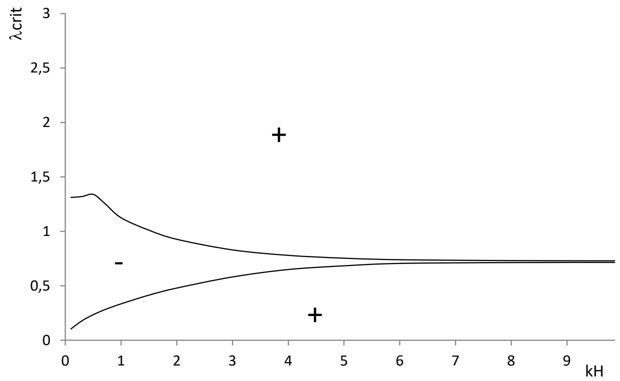

d)

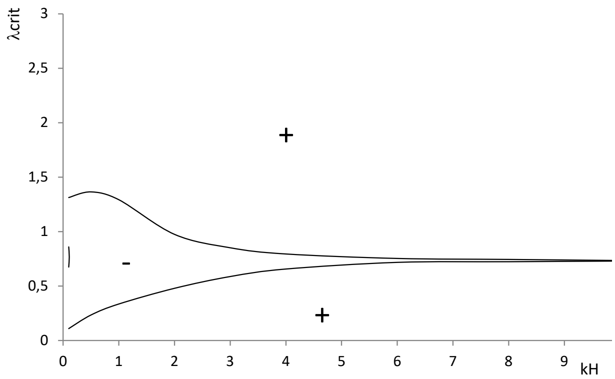

e)

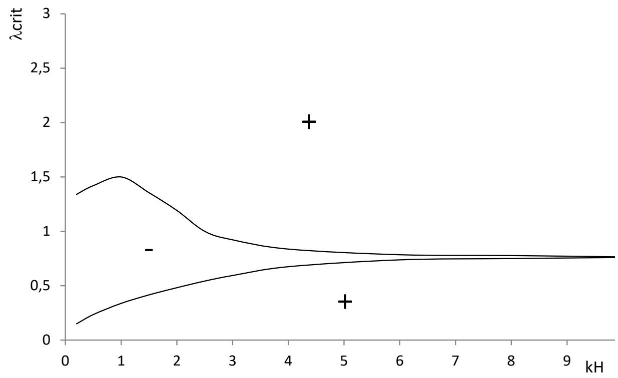

f)

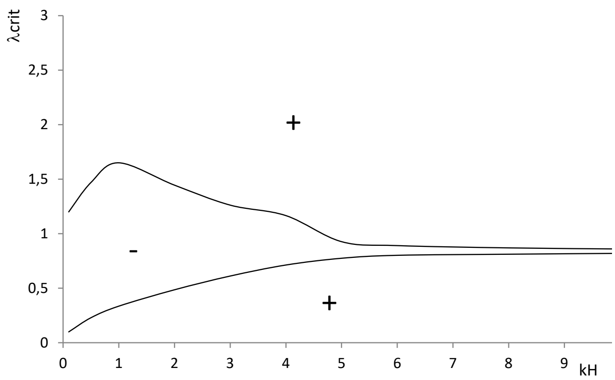

g)

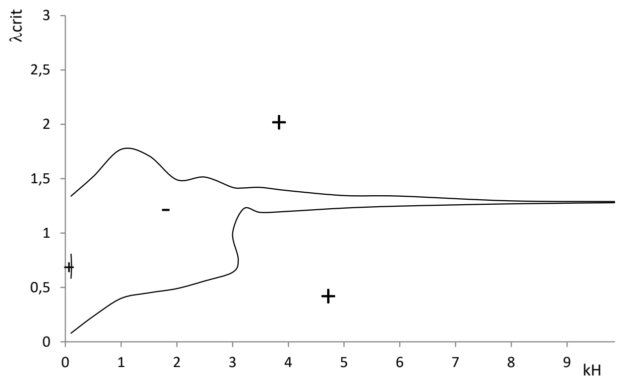

h)

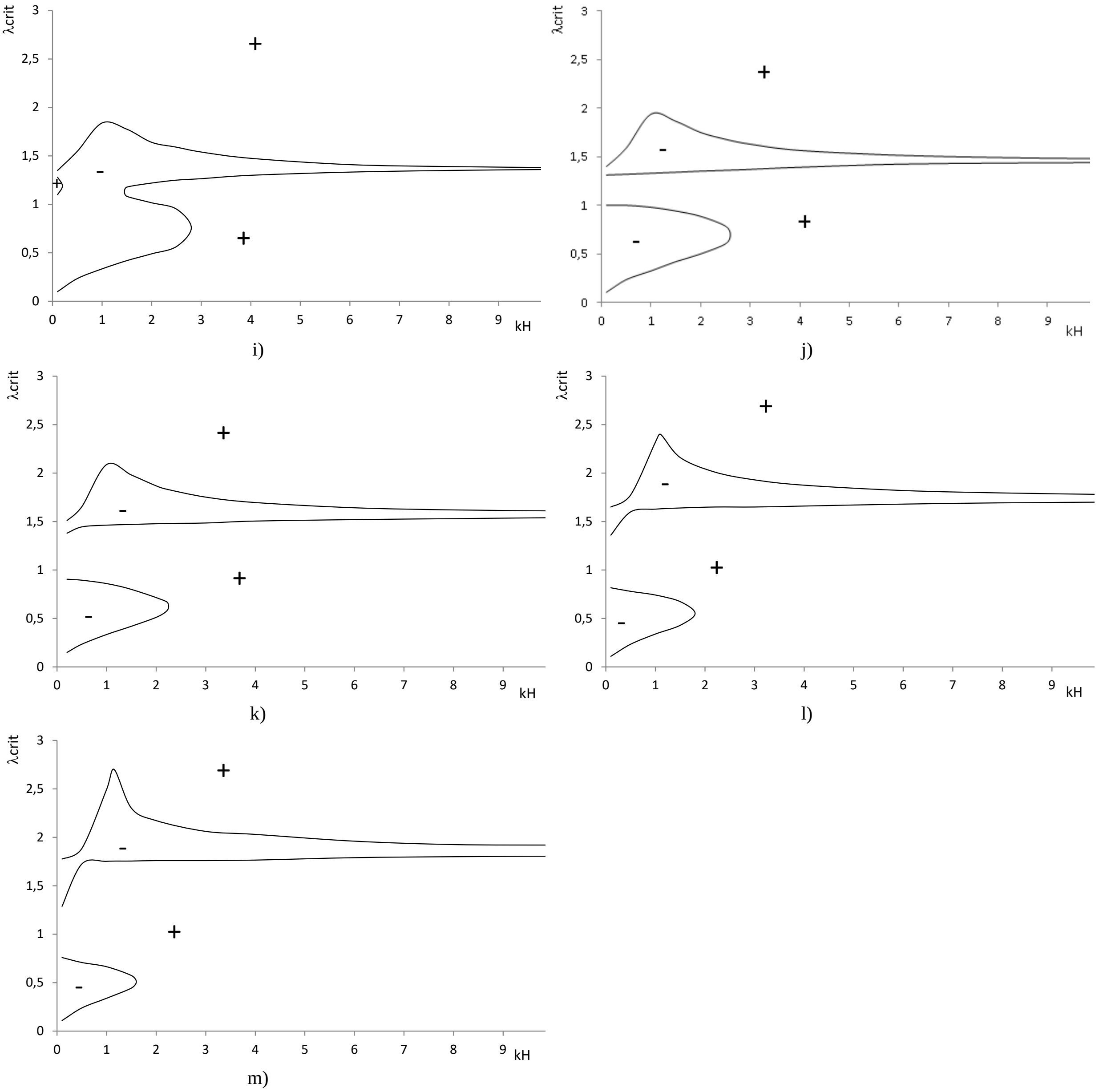

Figure 7. Plots of λ_{cr} vs kH for the Ogden model with values of $\widehat{D}_2$=0, 0.1, 0.5, 1, 1.15, 1.4, 1.7, 2, 2.2, 2.5, 3, 4 and 5 in (a)-(m) respectively. (+) indicates stable behaviour and (-) unstable behaviour.

Figure(s)

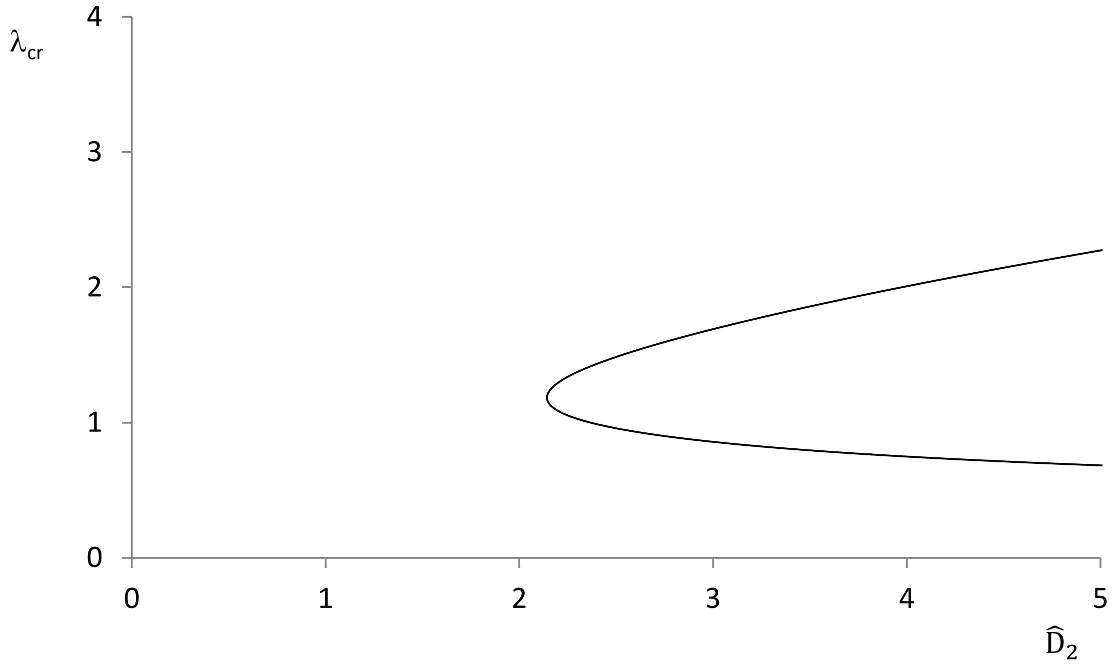

Figure 8. Plot of λ_{cr} versus $\hat{D}_2$ for β=0.5

Figure(s)

Figure captions

Figure 1. Plot of $\widehat{D}_2$ vs λ for β=0.5 and $\text{m}\Omega_1^* = \pm 0.01$.

Figure 2. Plot of $\text{m}\Omega_1^*$ vs λ for β=0,5 and $\widehat{D}_2$=0, 0.1, 0.5, 1, 1.7, 1.9, 2, 3, 4, 5.

Figure 3. Plots of λ_{cr} vs kH, $\text{m}\Omega_1^* = 0.01$ and $h^* = 0.2$ with values of $\widehat{D}_2$=0, 0.1, 0.5, 1, 1.7, 1.9, 2, 3, 4 and 5 in (a)-(j) respectively. (+) indicates stable behaviour and (-) unstable behaviour.

Figure 4. Plots of λ_{cr} vs kH, $\text{m}\Omega_1^* = -0.01$ and $h^* = 0.2$ with values of $\widehat{D}_2$=0, 0.1, 0.5, 1, 1.25, 1.5, 1.7, 1.85, 1.89, 1.925 , 2, 2.1, 2.25, 2.5, 3, 4 and 5 in (a)-(r) respectively. (+) indicates stable behaviour and (-) unstable behaviour.

Figure 5. Plots of λ_{cr} vs kH for the modified Mooney-Rivlin model, $\text{m}\Omega_1^* = 0$ and $h^* = 0.2$ with values of $\widehat{D}_2$=0, 0.5, 1, 1.5, 1.7, 2, 3, 4 and 5 in (a)-(j) respectively. (+) indicates stable behaviour and (-) unstable behaviour.

Figure 6. Plot of $\text{m}\Omega_1^*$ vs λ for several values of $\widehat{D}_2$

Figure 7. Plots of λ_{cr} vs kH for the Ogden model with values of $\widehat{D}_2$=0, 0.1, 0.5, 1, 1.15, 1.4, 1.7, 2, 2.2, 2.5, 3, 4 and 5 in (a)-(m) respectively. (+) indicates stable behaviour and (-) unstable behaviour.

Figure 8. Plot of λ_{cr} versus $\widehat{D}_2$ for β=0.5